Mon. Not. R. Astron. Soc. **000**, 1–20 (2012) Printed 25 September 2012 (MN LATEX style file v2.2)

Event rates for extreme-mass-ratio bursts from the Galactic Centre

C. P. L. Berry[1⋆] and J. R. Gair[1]
[1] *Institute of Astronomy, University of Cambridge, Madingley Road, Cambridge, CB3 0HA*

25 September 2012

ABSTRACT
I thought I would try out the MNRAS LATEX style.

Key words: black hole physics – celestial mechanics – Galaxy: centre – gravitational waves.

1 INTRODUCTION

The most compelling evidence for the existence of astrophysical black holes (BHs) come from the measurement of stellar orbits at the centre of the Galaxy. The stars are found to orbit an object of mass $M_\bullet \simeq 4 \times 10^6 M_\odot$ coincident with the compact radio source Sagittarius A* (Reid & Brunthaler 2004; Ghez et al. 2008; Gillessen et al. 2009). This is the nearest member of a population massive black holes (MBHs; Volonteri 2010) that are believed to occupy the centre of galaxies (Lynden-Bell 1969; Lynden-Bell & Rees 1971; Rees 1984; Ferrarese & Ford 2005). The Galactic Centre is an ideal laboratory for investigating the properties of an MBH and its surrounding nuclear star cluster (Genzel et al. 2010).

One means of investigating the properties of MBHs is through gravitational waves (GWs). A stellar mass compact object (CO), such as a main sequence (MS) star, white dwarf (WD), neutron star or stellar mass BH, emits gravitational radiation as it orbits the MBH. On account of the extreme-mass-ratio between the two bodies, we can approximate the CO as moving in the background spacetime of the MBH.

A space-borne detector, such as the *Laser Interferometer Space Antenna* (*LISA*) or the *evolved Laser Interferometer Space Antenna* (*eLISA*), is designed to be able to detect GWs in the frequency range of interest for these encounters (Bender et al. 1998; Danzmann & Rüdiger 2003; Jennrich et al. 2011; Amaro-Seoane et al. 2012). There are currently no funded space-borne detector missions. However, the European Space Agency's *LISA Pathfinder* will launch in 2014 and demonstrate the key technologies required for successful space-borne mission (Anza et al. 2005; Antonucci et al. 2012).

The gravitational waveforms emitted from these extreme-mass-ratio systems have been much studied (Glampedakis 2005; Barack 2009). The GWs carry away energy and angular momentum, causing the orbit to shrink until eventually the object plunges into the MBH. The primary focus has been upon the later stages of the orbital evolution, immediately preceding plunge. By this stage, the orbit has circularised and emits continuously within the detector's frequency band. These signals are extreme mass-ratio inspirals (EMRIs; Amaro-Seoane et al. 2007). EMRIs can be observed over many orbits, allowing exquisitely high signal-to-noise ratios (SNRs) to accumulate. This makes them excellent probes of the background spacetime.

EMRIs evolve form more eccentric orbits. These initial orbits may be the results of scattering from two-body encounters. Rather than emitting a continuously detectable signal, highly eccentric orbits only emit significant radiation in a burst around the point of closest approach to the MBH. These are extreme mass-ratio bursts (EMRBs; Rubbo, Holley-Bockelmann, & Finn 2006).

EMRBs are much shorter in duration than EMRIs. This means they do not accumulate as high SNRs, or produce as detailed maps of the spacetime. They are therefore less valued prizes. However, they may still be an interesting signal. As an object inspirals it emits many bursts before eventually settling into a low eccentricity EMRI. Some obejcts will be scattered by two-body encounters and never reach the EMRI phase (Alexander & Hopman 2003). Thus, there are many EMRBs per EMRI, although this does not necessarily translate to there being more detectable EMRBs that EMRIs.

For EMRBs to be a useful astronomical signal we require three things: that the bursts contain sufficient information to improve our knowledge of their source systems; that their event rate is sufficiently high that we could expect to observe them over a mission life time, and that the signals can be successfully extracted from the data stream.

We have previous addressed the first concern: EMRBs can give good constraints on the key parameters describing the Galaxy's MBH if the periapse distance is $r_\mathrm{p} \lesssim 10 r_\mathrm{g}$, where $r_\mathrm{g} = GM_\bullet/c^2$ is a gravitational radius. This would allow us to improve upon the current uncertainty in the mass measurement of 8% (Gillessen et al. 2009). In addition, we could also measure the spin magnitude to a precision of 0.1.

⋆ E-mail: cplb2@cam.ac.uk

The second concern shall be the subject of this work. Previously, the best estimate for the event rate was Hopman, Freitag, & Larson (2007). They estimated that the event rate for *LISA* was $\sim 1\ \mathrm{yr}^{-1}$. We follow a similar approach, but significantly, we improve the calculation of SNR by using numerical kludge waveforms. In addition to this, we extend the analysis by not only considering the number of events that would be detectable, but also how many would be informative.

2 WAVEFORMS AND PARAMETER UNCERTAINTIES

3 EVENT RATES

3.1 The distribution function

We wish to calculate the probability that there is an encounter between a compact object on an orbital trajectory described by eccentricity e and periapse radius r_p and the massive black hole (MBH) at the galactic centre. To do so we must assume a particular distribution of stars. We begin by following the work of Bahcall & Wolf (1976, 1977) and assuming that the distribution function (DF) within the galactic core is just a function of the orbital energy (Shapiro & Marchant 1978); we define the energy per unit mass of the orbit as

$$\mathcal{E} = \frac{v^2}{2} - \frac{GM_\bullet}{r} \tag{1}$$

where $M_\bullet$ is the mass of the MBH. The number of stars is given by

$$N = \int \mathrm{d}^3 r \int \mathrm{d}^3 v f(\mathcal{E}). \tag{2}$$

Close to the centre of the galactic core, dynamics are dominated by the influence of the MBH as it is significantly more massive than the surrounding stars. We define its radius of influence as (Frank & Rees 1976)

$$r_\mathrm{c} = \frac{GM_\bullet}{\sigma^2} \tag{3}$$

where σ^2 is the line-of-sight velocity dispersion. We shall assume that the mass of stars enclosed within the radius is greater than the black hole mass, which is much greater than the mass of a typical star $M_\star$ (Bahcall & Wolf 1976). We define a reference number density $n_\star$ from the enclosed mass $m(r)$ such that

$$m_\star(r_\mathrm{c}) = \frac{4\pi r_\mathrm{c}^3}{3} n_\star M_\star. \tag{4}$$

Within the core, the distribution function can be calculated using the approximation of Fokker-Planck formalism (Binney & Tremaine 2008, section 7.4). The population of bound stars is evolved numerically until a steady state is reached: the unbound stars form a reservoir with an assumed Maxwellian distribution. Denoting a species of star by its mass M,

$$f_M(\mathcal{E}) = \frac{C_M n_\star}{(2\pi\sigma_M^2)^{3/2}} \exp\left(-\frac{\mathcal{E}}{\sigma_M^2}\right), \quad \mathcal{E} > 0, \tag{5}$$

where C_M is a normalisation constant.[1] If different stellar species are in equipartition, as was assumed by Bahcall & Wolf (1976, 1977), then we expect

$$M\sigma_M^2 = M_\star \sigma_\star^2. \tag{6}$$

However, if the unbound stellar population has reached equilibrium by violent relaxation, then all mass groups are expected to have similar velocity dispersions:

$$\sigma_M = \sigma_\star = \sigma, \tag{7}$$

and we have equipartition of energy per unit mass (Lynden-Bell 1967). This is assumed here following Alexander & Hopman (2009) and O'Leary et al. (2009). The steady-state distribution function is largely insensitive to this choice (Bahcall & Wolf 1977; Alexander & Hopman 2009).

For bound orbits, the DF can be approximated as a power law (Peebles 1972)

$$f_M(\mathcal{E}) = \frac{k_M n_\star}{(2\pi\sigma^2)^{3/2}} \left(-\frac{\mathcal{E}}{\sigma^2}\right)^{p_M}, \quad \mathcal{E} < 0. \tag{8}$$

The exponent p_M varies depending upon the mass of the object, determining mass segregation. For a system with a single mass component $p = 1/4$ (Bahcall & Wolf 1976; Young 1977). The normalisation constant k_M reflects the relative abundances of the different species.[2]

These cusp profiles should exist if the system has had sufficient time to become gravitationally relaxed. There is current debate about whether this may be the case, both for the Galactic centre and galaxies in general. This is discussed further in Appendix A6. For concreteness, we assume that a cusp has formed. If a cusp has not formed, we expect there to be a shallower core profile, with fewer objects passing close to the MBH. Our results are therefore an upper bound on possible event rates (Merritt 2010; Gualandris & Merritt 2012).

3.2 Model parameters

We shall use the Fokker-Planck model of Hopman & Alexander (2006a,b); Alexander & Hopman (2009). This includes four stellar species: main sequence (MS) stars, white dwarfs (WDs), neutron stars (NSs), and black holes (BHs). Their properties are summarised in table 1. The behaviour of the Fokker-Planck model has been verified by N-body simulations (Baumgardt et al. 2004; Preto & Amaro-Seoane 2010). The steeper power law for black holes means that they segregate about the MBH: they dominate in place of main sequence stars for radii $r < 10^{-4} r_\mathrm{c}$.

Binaries may form in the galactic centre, encouraged by its high stellar density (O'Leary et al. 2009). However the binary fraction is still expected to be small (Hopman 2009).

[1] C_M determines the population ratios of species M far from the black hole (Alexander & Hopman 2009).

[2] For a single mass population ($p = 1/4$) $k = 2C$ gives a fit correct to within a factor of two (Bahcall & Wolf 1976; Keshet et al. 2009), we assume this holds for the dominant species of stars as, although it shall change slightly with p, variation is small compared to errors introduced by fitting a simple power law (Hopman & Alexander 2006a; Alexander & Hopman 2009).

Table 1. Stellar model parameters for the galactic centre using the results of Alexander & Hopman (2009) We use the main sequence star as our reference. The number fractions for unbound stars are estimates corresponding to a model of continuous star formation (Alexander 2005); O'Leary et al. (2009) arrive at the same proportions.

Star	$M/M_\odot$	$C_M/C_\star$	p_M	$k_M/k_\star$ [a]
MS	1.0	1	−0.1	1
WD	0.6	0.1	−0.1	0.09
NS	1.4	0.01	0.0	0.01
BH	10	0.001	0.5	0.008

[a] Toonen et al. (2009)

Consequently, and because binaries shall be disrupted by the MBH for periapses smaller than

$$r_{\rm B} \simeq \left(\frac{M_\bullet}{M_1+M_2}\right)^{1/3} a_{\rm B}, \tag{9}$$

where M_1 and M_2 are the masses of the binary's components, and $a_{\rm B}$ is the binary's semi-major axis [cf. (29) below], we shall ignore the possible presence of binaries.

We assume a black hole mass of $M_\bullet = (4.31 \pm 0.36) \times 10^6 M_\odot$ (Gillessen et al. 2009) and a velocity dispersion of $\sigma = (103 \pm 20)\ \mathrm{km\,s^{-1}}$ (Tremaine et al. 2002). This gives a core radius of $r_{\rm c} = (1.7 \pm 0.7)$ pc. Using the results of Ghez et al. (2008) we would expect the total mass of stars core to be $m_\star(r_{\rm c}) = 6.4 \times 10^6 M_\odot$, which is within 5% of the value obtained similarly from Genzel et al. (2003). This gives a reference stellar density of $n_\star = 2.8 \times 10^5\ \mathrm{pc}^{-3}$.

3.3 Parametrising in terms of eccentricity & periapsis

We will characterise orbits by their eccentricity e and periapse radius $r_{\rm p}$. The latter, unlike the semimajor axis, is always well defined regardless of eccentricity. For Keplerian orbits, the energy $\mathcal{E}$ and angular momentum $\mathcal{J}$ per unit mass are entirely characterised by these parameters

$$\mathcal{E} = -\frac{GM_\bullet(1-e)}{2r_{\rm p}}, \tag{10}$$

$$\mathcal{J}^2 = GM_\bullet(1+e)r_{\rm p}. \tag{11}$$

The distribution function, however, is defined per element of phase space: it is necessary to change variables from position and velocity to eccentricity and periapsis. We start by decomposing the velocity into three orthogonal components: radial v_r, azimuthal v_ϕ and polar v_θ. We assume that the galactic core is spherically symmetric (Genzel et al. 2003; Schödel et al. 2007), therefore we are only interested in the combination

$$v_\perp^2 = v_\phi^2 + v_\theta^2 = v^2 - v_r^2. \tag{12}$$

Under this change of variables

$$\mathrm{d}^3v = \mathrm{d}v_r \mathrm{d}v_\phi \mathrm{d}v_\theta \to 2\pi v_\perp\, \mathrm{d}v_r\, \mathrm{d}v_\perp. \tag{13}$$

The specific energy and angular momentum are given by

$$\mathcal{E} = \frac{v_r^2+v_\perp^2}{2} - \frac{GM_\bullet}{r}, \tag{14}$$

$$\mathcal{J}^2 = r^2 v_\perp^2. \tag{15}$$

Combining these with our earlier expressions in terms of e and $r_{\rm p}$, we find

$$v_\perp^2 = \frac{GM_\bullet(1+e)r_{\rm p}}{r^2},$$

$$v_r^2 = GM_\bullet\left[\frac{2}{r} - \frac{(1-e)}{r_{\rm p}} - \frac{(1+e)r_{\rm p}}{r^2}\right]. \tag{16}$$

From the latter we can verify that the turning points of an orbit occur at

$$r = r_{\rm p},\ \frac{1+e}{1-e}r_{\rm p}; \tag{17}$$

the periapse is the only turning point for orbits with $e > 1$. Since we now have expressions for $\{v_r, v_\perp\}$ in terms of $\{e, r_{\rm p}\}$, we can calculate the Jacobian

$$\left|\frac{\partial(v_r, v_\perp)}{\partial(e, r_{\rm p})}\right| = \frac{1}{2v_r v_\perp}\frac{e}{r_{\rm p}}\left(\frac{GM_\bullet}{r}\right)^2. \tag{18}$$

Using this, we may rewrite our velocity element as

$$\mathrm{d}^3v \to \frac{\pi e}{v_r r_{\rm p}}\left(\frac{GM_\bullet}{r}\right)^2 \mathrm{d}e\, \mathrm{d}r_{\rm p}. \tag{19}$$

As a consequence of our assumed spherical symmetry, the volume element is

$$\mathrm{d}^3r = 4\pi r^2\, \mathrm{d}r. \tag{20}$$

Thus, the phase space volume element can be expressed

$$\mathrm{d}^3r\mathrm{d}^3v = \frac{4\pi^2(GM_\bullet)^2 e}{v_r r_{\rm p}}\, \mathrm{d}r\, \mathrm{d}e\, \mathrm{d}r_{\rm p}. \tag{21}$$

The number of stars in an element $\mathrm{d}r\, \mathrm{d}e\, \mathrm{d}r_{\rm p}$ is

$$n(r, e, r_{\rm p}) = \frac{4\pi^2(GM_\bullet)^2 e}{v_r r_{\rm p}} f(\mathcal{E}). \tag{22}$$

From this, we can construct the expected number of stars to be on orbits defined by $\{e, r_{\rm p}\}$. We will define this locally, allowing it to vary with position. The number of stars found in a small radius range δr with given orbital properties can be calculated by multiplying the total number of stars with these properties by the relative amount of time they spend in that range

$$n(r, e, r_{\rm p})\delta r = N(e, r_{\rm p}; r)\frac{\delta t}{P(e, r_{\rm p})} \tag{23}$$

where $N(e, r_{\rm p}; r)$ is the total number of stars with orbits given by $\{e, r_{\rm p}\}$ defined at r, δt is the time spent in δr and $P(e, r_{\rm p})$ is the period of the orbit. We will defer the definition of this time for unbound orbits for now. The time spent in the radius range is

$$\delta t = 2\frac{\delta r}{v_r}, \tag{24}$$

where the factor of 2 is included to account for both inwards and outwards motion. Hence

$$N(e, r_{\rm p}; r) = \frac{1}{2}v_r P(e, r_{\rm p}) n(r, e, r_{\rm p}) \tag{25}$$

$$= \frac{2\pi^2(GM_\bullet)^2 e P(e, r_{\rm p})}{r_{\rm p}} f(\mathcal{E}). \tag{26}$$

The right hand side of this equation is independent of position, subject to the constraint that the radius is in the allowed range for the orbit $r_{\rm p} \leqslant r \leqslant (1+e)r_{\rm p}/(1-e)$, and so we can define $N(e, r_{\rm p}) \equiv N(e, r_{\rm p}; r)$. This is a consequence

of the distribution function being dependent only upon a constant of the motion.[3]

If a burst of radiation is emitted each time a star passes through periapse, then the event rate for burst emission from orbits with parameters $\{e, r_\mathrm{p}\}$, is given by

$$\Gamma(e, r_\mathrm{p}) = \frac{N(e, r_\mathrm{p})}{P(e, r_\mathrm{p})} \tag{27}$$

$$= \frac{2\pi^2 (GM_\bullet)^2 e}{r_\mathrm{p}} f(\mathcal{E}). \tag{28}$$

The orbital period drops out from the calculation, so we do not have to worry about an appropriate definition for unbound orbits.

To generate a representative sample for the orbital parameters e and r_p, we use $\Gamma(e, r_\mathrm{p})$ as an unnormalised probability distribution and draw from it appropriately.

3.4 The inner cut-off

From (28) we see that the event rate is highly sensitive to the smallest value of the periapsis. The inner cut-off for r_p could result from a number of different physical causes. Ultimately the orbits cannot encroach closer to the MBH than its last stable orbit. This depends upon the spin of the MBH, but is of the order of its Schwarzschild radius. Before we reach this point, there are other processes that may intervene to deplete the orbiting stars. Our treatment of these is approximate, but should hopefully produce reasonable estimates. We consider three processes: tidal disruption by the MBH, gravitational wave inspiral and collisional disruption. Tidal disruption imposes a definite (albeit approximate) cut-off, while the others use statistical arguments; they are therefore true for a typical star, and it is unlikely that a star would be found beyond the imposed limits. For these methods, we will need to define a reference time-scale for relaxation, over which two-body interactions lead to significant changes in the orbital properties of the star. This is done in Sec. 3.4.2, with further details found in Appendix A.

The calculated inner cut-offs for the four stellar species are shown in fig. 1.

3.4.1 Tidal disruption

Tidal forces from the MBH can disrupt stars. This occurs at the tidal radius

$$r_\mathrm{T} \simeq \left(\frac{M_\bullet}{M}\right)^{1/3} R_M \tag{29}$$

where R_M is the radius of the star (Hills 1975; Rees 1988; Kobayashi et al. 2004).[4] Any star on an orbit with $r_\mathrm{p} < r_\mathrm{T}$ is disrupted in the course of its orbit. Parametrising orbits by their periapsis allows us to easily determine which stars should be disrupted. We do not include the full effects of the loss cone (Frank & Rees 1976; Lightman & Shapiro 1977; Cohn & Kulsrud 1978) as these were not incorporated into the Fokker-Planck calculations (Hopman 2009).[5]

[3] See Bahcall & Wolf (1976), equation (9) for a similar result.
[4] See Kesden (2012) for a general relativistic treatment.
[5] The loss cone is a region in velocity space where orbits are depleted because stars are disrupted more rapidly than they can be replenished by two-body scattering.

The effect of the loss cone should be small, only modifying the DF by a logarithmic term (Lightman & Shapiro 1977; Bahcall & Wolf 1977; Cohn & Kulsrud 1978). Its effects are diluted by resonant relaxation (Hopman et al. 2007; Toonen et al. 2009; Merritt et al. 2011). Furthermore, the loss cone could be refilled by the wandering of the MBH because of perturbations from the inhomogeneities in the stellar potential (Sigurdsson & Rees 1997; Chatterjee et al. 2002; Merritt et al. 2007).

Tidal disruption is significant for MS stars since they are least dense: calculated in this way, only MS stars would be tidally disrupted outside of the MBH's event horizon (Sigurdsson & Rees 1997). The tidal radius defines the cut-off for periapsis of high eccentricity ($e \gtrsim 1$) orbits (Lightman & Shapiro 1977).

3.4.2 Relaxation time-scale

The motion of a star is determined not only by the dominant influence of the central MBH, but also by the other stars. The gravitational potential of the stars may be split into two components: a smooth background representing the average distribution of stars, and statistical fluctuations from random deviations in the stellar distribution. The former only contributes to the stars' orbits: we neglect this since we are more interested in the influence of the MBH. The latter may be approximated as a series of two-body encounters. These lead to scattering, in a manner much like Brownian motion (Bekenstein & Maoz 1992; Maoz 1993; Nelson & Tremaine 1999).

The two-body interactions mostly lead to small deflections. Over time, these may accumulate into a significant change in the dynamics. The relaxation time-scale characterises the time taken for this to happen (Binney & Tremaine 2008, section 1.2.1). It therefore quantifies the time over which an orbit may be repopulated by scattering. There are a variety of definitions for the relaxation time-scale. For a system with a purely Maxwellian distribution, the time-scale has form

$$\tau_\mathrm{R}^\mathrm{Max} \simeq \kappa \frac{\sigma^3}{G^2 M_\star^2 n_\star \ln\Lambda}, \tag{30}$$

where the Coulomb logarithm is $\ln\Lambda = \ln(M_\bullet/M_\star)$ (Bahcall & Wolf 1976), and κ is a dimensionless number. In his pioneering work, Chandrasekhar (1941b, 1960) defined the time-scale as the period over which the squared change in energy was equal to the kinetic energy squared, this gives $\kappa = 9/16\sqrt{\pi} \simeq 0.32$. Subsequently, Chandrasekhar (1941a) described relaxation statistically, treating fluctuations in the gravitational field probabilistically; this gives $\kappa = 9/2(2\pi)^{3/2} \simeq 0.29$. Bahcall & Wolf (1977) define a reference time-scale from their Boltzmann equation with $\kappa = 3/4\sqrt{8\pi} \simeq 0.15$; this is equal to the reference time-scale defined as the reciprocal of the coefficient of dynamical friction by Chandrasekhar (1943a,b). Spitzer & Harm (1958) define a reference time-scale from the gravitational Boltzmann equation of Spitzer & Schwarzschild (1951) where $\kappa = \sqrt{2}/\pi \simeq 0.45$. Following Spitzer & Hart (1971), Binney & Tremaine (2008, section 7.4.5) estimate the time-scale from the velocity diffusion coefficient of the Fokker-Planck equation yielding $\kappa \simeq 0.34$.

All these approaches yield consistent values, suggesting,

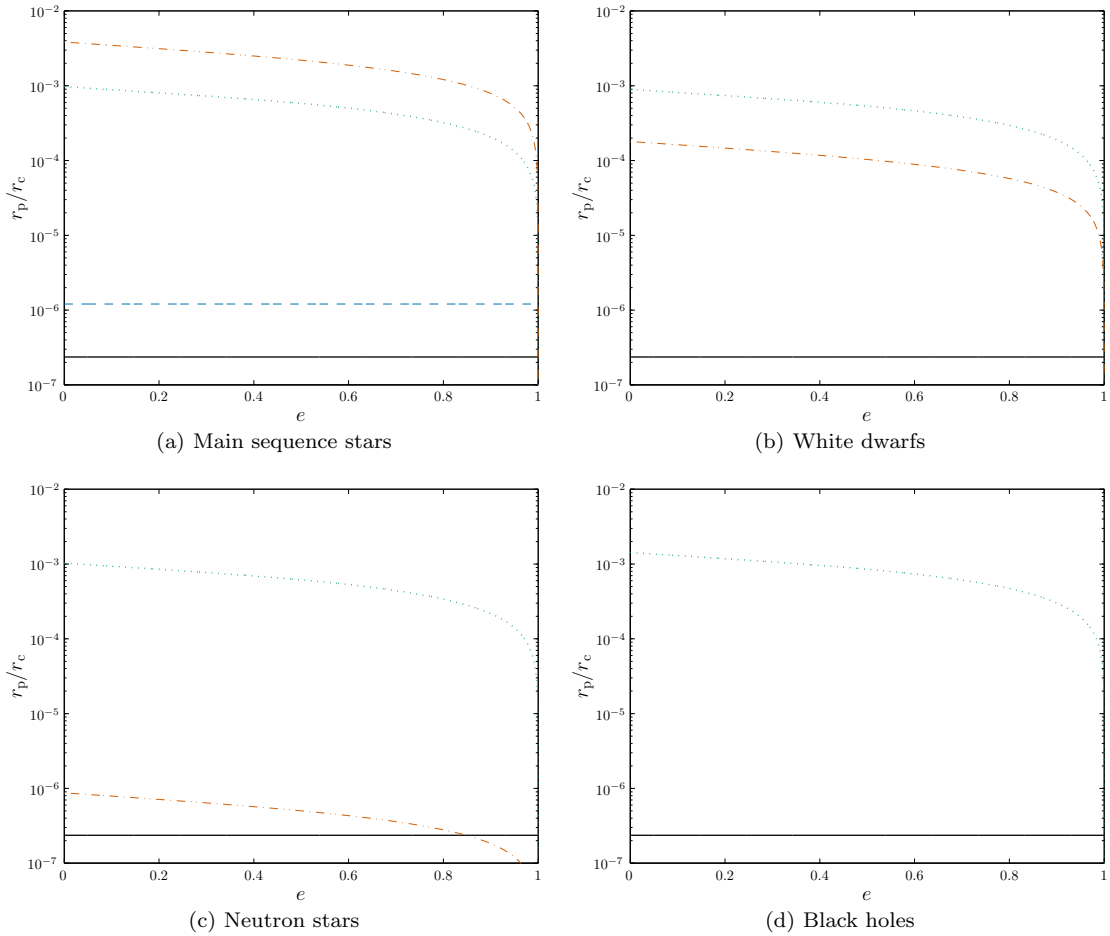

(a) Main sequence stars (b) White dwarfs

(c) Neutron stars (d) Black holes

Figure 1. Inner cut-off radii for the Galactic Centre as a function of eccentricity. The solid line is the Schwarzschild radius of the MBH; the dashed line is the tidal radius; the dot-dashed line is the collisional cut-off, and the dotted line is the transition to the GW-dominated inspiral regime.

as a first approximation, any should be valid. We will follow the classic treatment of Chandrasekhar (1960, chapter 2) which is transparent in its assumptions, adapting from a Maxwellian distribution of velocities to one derived from the DFs (5) and (8). This, at least, makes the model self-consistent. Since there is uncertainty in the astrophysical parameters, we will not be concerned by small discrepancies in the numerical prefactor that result from the simplifying approximations of this approach. The derivation of the relaxation time-scale along with a discussion of its short-comings are included in Appendix A. An average time-scale for the entire system is defined in (A80), and an average for an orbit is defined in (A94). We defer any investigation of the consequences of using an alternative formulation for future work, as differences may well be negligible whilst the computation can be complicated.

Two-body interactions lead to diffusion in both energy and angular momentum. When considering a single (bound) orbit, over a relaxation time-scale the energy changes by order of itself while the angular momentum changes by the angular momentum of a circular orbit with that energy $\mathcal{J}_\mathrm{circ}(\mathcal{E})$ (Lightman & Shapiro 1977; Rauch & Tremaine 1996; Hopman & Alexander 2005):[6]

$$\left(\frac{\Delta\mathcal{E}}{\mathcal{E}}\right)^2 \approx \left[\frac{\Delta\mathcal{J}}{\mathcal{J}_\mathrm{circ}(\mathcal{E})}\right]^2 \approx \frac{t}{\tau_\mathrm{R}}. \tag{31}$$

We may define another angular momentum relaxation time-scale as the time taken for the angular momentum to change by order of itself (Merritt et al. 2011)

$$\tau_\mathcal{J} = \left[\frac{\mathcal{J}}{\mathcal{J}_\mathrm{max}(\mathcal{E})}\right]^2 \tau_\mathrm{R} \tag{32}$$

$$= \left(1-e^2\right)\tau_\mathrm{R}. \tag{33}$$

This can be much shorter than the energy relaxation time-scale: diffusion in angular momentum can proceed more rapidly than diffusion in energy.

3.4.3 Gravitational wave inspiral

Stars orbiting about the MBH continually emit gravitational radiation; this carries away energy and angular momentum, causing the stars to inspiral. Using the analysis of Peters & Mathews (1963) and Peters (1964) for

[6] The circular-orbit angular momentum is the maximum value for orbits of that energy.

Keplerian binaries it is possible to define a characteristic inspiral time-scale from the rate of change of energy. For consistency with the definition of the relaxation time-scale, we define the characteristic inspiral time-scale as (Miralda-Escude & Gould 2000; Merritt et al. 2011)

$$\tau_{\rm GW} \simeq \mathcal{E}\left\langle \frac{\mathrm{d}\mathcal{E}}{\mathrm{d}t}\right\rangle^{-1}, \tag{34}$$

where the term in angular brackets is the orbit-averaged rate of energy radiation. Using (10) and equation (16) of Peters & Mathews (1963)

$$\begin{aligned}\tau_{\rm GW} &\simeq \frac{5}{64}\frac{c^5 r_{\rm p}^4}{G^3 M M_\bullet (M+M_\bullet)}\frac{(1+e)^{7/2}}{(1-e)^{1/2}} \\ &\quad\times\left(1+\frac{73}{24}e^2+\frac{37}{96}e^4\right)^{-1} \qquad (35)\\ &\approx \frac{5}{64}\frac{c^5 r_{\rm p}^4}{G^3 M M_\bullet^2}\frac{(1+e)^{7/2}}{(1-e)^{1/2}}\left(1+\frac{73}{24}e^2+\frac{37}{96}e^4\right)^{-1}. \qquad (36)\end{aligned}$$

For comparison, the total time taken for the inspiral, if undisturbed, is given in (B8). The characteristic time-scale is a better measure of the depletion of an orbit as it only depends upon the parameters of that orbit, and not its future evolution.

The time-scale associated with changes in angular momentum is (Peters 1964)

$$\begin{aligned}\tau_{{\rm GW},\mathcal{J}} &\simeq \mathcal{J}\left\langle\frac{\mathrm{d}\mathcal{J}}{\mathrm{d}t}\right\rangle^{-1} \qquad (37)\\ &\simeq \frac{5}{32}\frac{c^5 r_{\rm p}^4}{G^3 M M_\bullet (M+M_\bullet)}\frac{(1+e)^{5/2}}{(1-e)^{3/2}}\left(1+\frac{7}{8}e^2\right)^{-1} \qquad (38)\\ &\approx \frac{5}{32}\frac{c^5 r_{\rm p}^4}{G^3 M M_\bullet^2}\frac{(1+e)^{5/2}}{(1-e)^{3/2}}\left(1+\frac{7}{8}e^2\right)^{-1}. \qquad (39)\end{aligned}$$

This is always greater than the energy time-scale; hence, we only consider changes in energy from gravitational wave emission as important for evolution of the system (Hopman & Alexander 2005).

Unbound stars only undergo a single periapse passage and only radiate one burst of radiation; we therefore neglect any evolution in their orbital parameters.[7]

The $(1-e)^{-1/2}$ dependence of $\tau_{\rm GW}$ for bound orbits connects the two regimes. The rate of change of energy goes to zero as a consequence of the assumption that the orbital parameters do not change over the course of a single orbit. This was necessary to calculate the orbit-averaged quantity. It is a valid approximation since the large mass-ratio ensures a slow evolution of the system (Appendix B2).

When comparing with the relaxation time-scale we are in effect comparing rates of change, with the shorter time-scale highlighting the more rapid process that will dominate the evolution (Amaro-Seoane et al. 2007). We shall therefore compare $\tau_{\rm GW}$ with the orbital relaxation time-scale $\tau_{\mathcal{J}}$ (Merritt et al. 2011). Orbits with inspiral time-scales shorter than orbital relaxation time-scales become depleted by gravitational wave emission faster than they are replenished by scattering. The cusp will not extend to these orbits. Yet, these orbits are not totally depopulated as an object may pass through during its inspiral from a greater periapse and eccentricity. The net effect is that the distributions of MS stars, WDs and NSs are relatively unchanged from their cusp states, but the BH population is significantly depleted.

[7] Using the analysis of Turner (1977) it is possible to show that the relative changes in eccentricity $\Delta e/e$ and periapsis $\Delta r_{\rm p}/r_{\rm p}$ for an extreme mass-ratio binary are less than $\sqrt{e}\,\mathcal{O}(\eta)$, where $\eta = M/M_\bullet$ is small, and so are only important for very high eccentricity orbits (Appendix B2). These are very high energy, and exponentially rare because of the Boltzmann factor in (5).

3.4.4 Collisions

As a consequence of the higher densities in the galactic core, stars may undergo a large number of close encounters with other stars (Cohn & Kulsrud 1978). These may lead to their destruction. MS stars, WDs, and NSs may be pulled apart by tidal forces if they stray too close to a a more massive object. As MS stars are diffuse, they would not tidally disrupt another star (Murphy et al. 1991; Freitag & Benz 2005), close encounters would result in some mass transfer; however, the cumulative effect of 20–30 grazing collisions could disrupt a MS star (Freitag et al. 2006). The number of collisions a star shall undergo in a time interval δt is

$$\delta K = n(r) A v(r, e, r_{\rm p})\delta t, \tag{40}$$

where A is the collisional cross-sectional area. For tidal disruption, where the encounter is with a collapsed object (WD, NS or BH), we set $A = \pi r_{\rm T}^{M'}$, where $r_{\rm T}^{M'}$ is the appropriate tidal radius: it is the same as (29) but with $M_\bullet$ replaced with the mass of the collapsed object M'. For collisions between MS stars, the cross-sectional area is simply the geometric $A = \pi R_\star^2$.[8]

For circular orbits we can find the radius at which collisions lead to disruptions by setting $\delta K = 1$ for tidal disruption or $\delta K = 20$ for grazing collisions, and $\delta t = \tau_{\rm R}$. We use the relaxation time-scale for the system as this is the time over which stars are replenished from the reservoir. For non-circular orbits we must consider variation with position. Using $\delta r = v_r \delta t$, and then converting to an integral, we have for bound orbits

$$K = 2A\frac{\tau_{\rm R}}{P(r_{\rm p}, e)}\int_{r_{\rm p}}^{(1+e)r_{\rm p}/(1-e)} n(r)\frac{v(r,e,r_{\rm p})}{v_r(r,e,r_{\rm p})}\,\mathrm{d}r, \tag{41}$$

where P is the period of the orbit. Again we may set $K = 1$ or $K = 20$ to find the orbits for which stars will be disrupted within a relaxation time-scale (of the system). For unbound orbits we are only interested in stars that would become disrupted before their periapse passage, so

$$K = A\int_{r_{\rm p}}^{r_{\rm c}} n(r)\frac{v(r,e,r_{\rm p})}{v_r(r,e,r_{\rm p})}\,\mathrm{d}r, \tag{42}$$

assuming that the stars in the reservoir external to the core are unlikely to undergo close collisions.

Collisions provide the cutoff for MS stars, and are significant for WDs.

[8] Here we assume that the relative velocity of the colliding stars is much greater than the escape velocity of the star so we may neglect the effects of gravitational focusing.

ACKNOWLEDGMENTS

The authors are grateful for insightful discussions with Sverre Aarseth. The authors thank Tal Alexander and Clovis Hopman for useful correspondence. CPLB is supported by STFC. JRG is supported by the Royal Society.

REFERENCES

Alexander T., 2005, Physics Reports, 419, 65
Alexander T., Hopman C., 2003, The Astrophysical Journal, 590, L29
Alexander T., Hopman C., 2009, The Astrophysical Journal, 697, 1861
Amaro-Seoane P. et al., 2012, Classical and Quantum Gravity, 29, 124016(20)
Amaro-Seoane P., Gair J. R., Freitag M., Miller M. C., Mandel I., Cutler C. J., Babak S., 2007, Classical and Quantum Gravity, 24, R113
Amaro-Seoane P., Preto M., 2011, Classical and Quantum Gravity, 28, 094017(14)
Antonucci F. et al., 2012, Classical and Quantum Gravity, 29, 124014(10)
Anza S. et al., 2005, Classical and Quantum Gravity, 22, S125
Bahcall J. N., Wolf R. A., 1976, The Astrophysical Journal, 209, 214
Bahcall J. N., Wolf R. A., 1977, The Astrophysical Journal, 216, 883
Bar-Or B., Kupi G., Alexander T., 2012, 20
Barack L., 2009, Classical and Quantum Gravity, 26, 213001(56)
Baumgardt H., Makino J., Ebisuzaki T., 2004, The Astrophysical Journal, 613, 1133
Bekenstein J. D., Maoz E., 1992, The Astrophysical Journal, 390, 79
Bender P. et al., 1998, LISA Pre-Phase A Report. Tech. rep., Max-Planck-Institut für Quantenoptik, Garching
Binney J., Tremaine S., 2008, Galactic Dynamics, 2nd edn., Princeton Series in Astrophysics. Princeton University Press, Princeton, New Jersey
Chandrasekhar S., 1941a, The Astrophysical Journal, 94, 511
Chandrasekhar S., 1941b, The Astrophysical Journal, 93, 285
Chandrasekhar S., 1941c, The Astrophysical Journal, 93, 323
Chandrasekhar S., 1943a, The Astrophysical Journal, 97, 255
Chandrasekhar S., 1943b, The Astrophysical Journal, 98, 54
Chandrasekhar S., 1960, Principles of Stellar Dynamics, enlarged edn. Dover Publications, New York
Chatterjee P., Hernquist L., Loeb A., 2002, The Astrophysical Journal, 572, 371
Cohn H., Kulsrud R. M., 1978, The Astrophysical Journal, 226, 1087
Danzmann K., Rüdiger A., 2003, Classical and Quantum Gravity, 20, S1
Eilon E., Kupi G., Alexander T., 2009, The Astrophysical Journal, 698, 641
Ferrarese L., Ford H., 2005, Space Science Reviews, 116, 523
Frank J., Rees M. J., 1976, Monthly Notices of the Royal Astronomical Society, 176, 633
Freitag M., Amaro-Seoane P., Kalogera V., 2006, The Astrophysical Journal, 649, 91
Freitag M., Benz W., 2005, Monthly Notices of the Royal Astronomical Society, 358, 1133
Genzel R., Eisenhauer F., Gillessen S., 2010, Reviews of Modern Physics, 82, 3121
Genzel R. et al., 2003, The Astrophysical Journal, 594, 812
Ghez A. M. et al., 2008, The Astrophysical Journal, 689, 1044
Gillessen S., Eisenhauer F., Trippe S., Alexander T., Genzel R., Martins F., Ott T., 2009, The Astrophysical Journal, 692, 1075
Glampedakis K., 2005, Classical and Quantum Gravity, 22, S605
Gualandris A., Merritt D., 2012, The Astrophysical Journal, 744, 74(21)
Gürkan M. A., Hopman C., 2007, Monthly Notices of the Royal Astronomical Society, 379, 1083
Hills J. G., 1975, Nature, 254, 295
Hopman C., 2009, The Astrophysical Journal, 700, 1933
Hopman C., Alexander T., 2005, The Astrophysical Journal, 629, 362
Hopman C., Alexander T., 2006a, The Astrophysical Journal, 645, 1152
Hopman C., Alexander T., 2006b, The Astrophysical Journal, 645, L133
Hopman C., Freitag M., Larson S. L., 2007, Monthly Notices of the Royal Astronomical Society, 378, 129
Jennrich O. et al., 2011, NGO Revealing a hidden Universe: opening a new chapter of discovery. Tech. rep., European Space Agency
Just A., Khan F. M., Berczik P., Ernst A., Spurzem R., 2011, Monthly Notices of the Royal Astronomical Society, 411, 653
Kesden M., 2012, Physical Review D, 85, 024037(9)
Keshet U., Hopman C., Alexander T., 2009, The Astrophysical Journal, 698, L64
Kobayashi S., Laguna P., Phinney E. S., Meszaros P., 2004, The Astrophysical Journal, 615, 855
Landau L. D., Lifshitz E. M., 1958, Statistical Physics, Course of Theoretical Physics. Pergamon Press, London
Li S., Liu F. K., Berczik P., Chen X., Spurzem R., 2012, The Astrophysical Journal, 748, 65
Lightman A. P., Shapiro S. L., 1977, The Astrophysical Journal, 211, 244
Lynden-Bell D., 1967, Monthly Notices of the Royal Astronomical Society, 136, 101
Lynden-Bell D., 1969, Nature, 223, 690
Lynden-Bell D., Kalnajs A., 1972, Monthly Notices of the Royal Astronomical Society, 157, 1
Lynden-Bell D., Rees M. J., 1971, Monthly Notices of the Royal Astronomical Society, 152, 461
Maoz E., 1993, Monthly Notices of the Royal Astronomical Society, 263, 75
Merritt D., 2010, The Astrophysical Journal, 718, 739
Merritt D., Alexander T., Mikkola S., Will C. M., 2011, Physical Review D, 84, 044024(21)
Merritt D., Berczik P., Laun F., 2007, The Astronomical

Journal, 133, 553
Miralda-Escude J., Gould A., 2000, The Astrophysical Journal, 545, 847
Mulder W., 1983, Astronomy and Astrophysics, 117, 9
Murphy B. W., Cohn H. N., Durisen R. H., 1991, The Astrophysical Journal, 370, 60
Nelson R. W., Tremaine S., 1999, Monthly Notices of the Royal Astronomical Society, 306, 1
O'Leary R. M., Kocsis B., Loeb A., 2009, Monthly Notices of the Royal Astronomical Society, 395, 2127
Olver F. W. J., Lozier Daniel W., Boisvert R. F., Clark C. W., eds., 2010, NIST Handbook of Mathematical Functions. Cambridge University Press, Cambridge, p. 968
Peebles P. J. E., 1972, The Astrophysical Journal, 178, 371
Peters P. C., 1964, Physical Review, 136, B1224
Peters P. C., Mathews J., 1963, Physical Review, 131, 435
Preto M., Amaro-Seoane P., 2010, The Astrophysical Journal, 708, L42
Rauch K. P., Ingalls B., 1998, Monthly Notices of the Royal Astronomical Society, 299, 1231
Rauch K. P., Tremaine S., 1996, New Astronomy, 1, 149
Rees M. J., 1984, Annual Review of Astronomy and Astrophysics, 22, 471
Rees M. J., 1988, Nature, 333, 523
Reid M. J., Brunthaler A., 2004, The Astrophysical Journal, 616, 872
Rubbo L. J., Holley-Bockelmann K., Finn L. S., 2006, The Astrophysical Journal, 649, L25
Schödel R. et al., 2007, Astronomy and Astrophysics, 469, 125
Shapiro S. L., Marchant A. B., 1978, The Astrophysical Journal, 225, 603
Sigurdsson S., Rees M., 1997, Monthly Notices of the Royal Astronomical Society, 284, 318
Spitzer L., Hart M. H., 1971, The Astrophysical Journal, 164, 399
Spitzer L., Shapiro S. L., 1972, The Astrophysical Journal, 173, 529
Spitzer, Jr. L., 1987, Dynamical Evolution of Globular Clusters, Princeton Series in Astrophysics. Princeton University Press, Princeton, New Jersey
Spitzer, Jr. L., Harm R., 1958, The Astrophysical Journal, 127, 544
Spitzer, Jr. L., Schwarzschild M., 1951, The Astrophysical Journal, 114, 385
Toonen S., Hopman C., Freitag M., 2009, Monthly Notices of the Royal Astronomical Society, 398, 1228
Tremaine S. et al., 2002, The Astrophysical Journal, 574, 740
Tremaine S., Weinberg M., 1984, Monthly Notices of the Royal Astronomical Society, 209, 729
Turner M., 1977, The Astrophysical Journal, 216, 610
Volonteri M., 2010, The Astronomy and Astrophysics Review, 18, 279
Weinberg M. D., 1986, The Astrophysical Journal, 300, 93
Wyse R., 2008, in ASP Conference Series, Vol. 399, Panoramic Views of Galaxy Formation and Evolution, Kodama T., Yamada T., Aoki K., eds., Astronomical Society of the Pacific, San Francisco, California, pp. 445–448
Young P. J., 1977, The Astrophysical Journal, 217, 287

APPENDIX A: CHANDRASEKHAR'S RELAXATION TIME-SCALE

Chandrasekhar (1960, chapter 2) defined a relaxation time-scale for a stellar system by approximating the fluctuations in the stellar gravitational potential as a series of two-body encounters. The time over which the squared change in energy is equal to the (initial) kinetic energy of the star is the time taken for relaxation. Relaxation is explained through dynamical friction (Chandrasekhar 1943a; Binney & Tremaine 2008, section 1.2). This can be understood intuitively as the drag induced on a star by the over-density of field stars deflected by its passage (Mulder 1983). In the interaction between the star and its gravitational wake, energy and momentum are exchanged, accelerating some stars, decelerating others.

Chandrasekhar's approach has proved exceedingly successful despite the number of simplifying assumptions inherent in the model which are not strictly applicable to systems such as the Galactic centre. We will not attempt to fix these deficiencies, rather, the only modification to the standard picture shall be to substitute the velocity distribution: while the canonical formulation uses a simple homogeneous Gaussian distribution, we use a distribution derived from the distribution functions (5) and (8).

Other authors have built upon the work of Chandrasekhar by considering inhomogeneous stellar distributions, via perturbation theory (Lynden-Bell & Kalnajs 1972; Tremaine & Weinberg 1984; Weinberg 1986); modelling energy transfer as anomalous dispersion, which adds higher order moments to the transfer probability (Bar-Or et al. 2012), or using the tools of linear response theory and the fluctuation-dissipation theory (Landau & Lifshitz 1958, chapter 7), which allows relaxation of certain assumptions, such as homogeneity (Bekenstein & Maoz 1992; Maoz 1993; Nelson & Tremaine 1999). We will not attempt to employ such sophisticated techniques at this stage.

A1 Chandrasekhar's derivation of the change in energy

We consider the interaction of a field star, denoted by 1, with a test star, 2; the centre-of-gravity and relative velocities are

$$\boldsymbol{V}_{\mathrm{g}} = \frac{1}{m_1+m_2}\left(m_1\boldsymbol{v}_1 + m_2\boldsymbol{v}_2\right); \tag{A1a}$$

$$\boldsymbol{V} = \boldsymbol{v}_1 - \boldsymbol{v}_2. \tag{A1b}$$

Hence

$$v_1^2 = V_{\mathrm{g}}^2 - 2\frac{m_2}{m_1+m_2}V_{\mathrm{g}}V\cos\Phi + \left(\frac{m_2}{m_1+m_2}\right)^2 V^2; \tag{A2a}$$

$$v_2^2 = V_{\mathrm{g}}^2 + 2\frac{m_1}{m_1+m_2}V_{\mathrm{g}}V\cos\Phi + \left(\frac{m_1}{m_1+m_2}\right)^2 V^2, \tag{A2b}$$

where Φ is the angle between $\boldsymbol{V}_{\mathrm{g}}$ and $\boldsymbol{V}$, and

$$V_{\mathrm{g}}^2 = \frac{1}{(m_1+m_2)^2}\left(m_1v_1^2 + m_2v_2^2 + 2m_1m_2v_1v_2\cos\theta\right); \tag{A3a}$$

$$V^2 = v_1^2 + v_2 - 2v_1v_2\cos\theta, \tag{A3b}$$

where θ is the angle between $\boldsymbol{v}_1$ and $\boldsymbol{v}_2$. The change in energy of during the interaction is

$$\Delta E = \frac{1}{2}m_2\left(v_2'^{\,2} - v_2^2\right) \tag{A4}$$

$$= \frac{m_1m_2}{m_1+m_2}V_{\mathrm{g}}V\left(\cos\Phi' - \cos\Phi\right), \tag{A5}$$

using primed variables for values after the interaction, and unprimed ones for before. If we project the angle out onto the orbital plane

$$\Delta E = \frac{m_1m_2}{m_1+m_2}V_{\mathrm{g}}V\left(\cos\phi' - \cos\phi\right)\cos i, \tag{A6}$$

where ϕ is the angle in the plane, and i is the inclination of $\boldsymbol{V}_{\mathrm{g}}$ out of the plane. We define the deflection angle ψ such that

$$\phi' - \phi = \pi - 2\psi, \tag{A7}$$

hence

$$\Delta E = -2\frac{m_1m_2}{m_1+m_2}V_{\mathrm{g}}V\cos(\phi-\psi)\cos\psi\cos i. \tag{A8}$$

We now need to calculate the encounter rate. This requires us to know number of field stars per unit volume and per volume space element. We make the simplifying assumption that the density of stars is uniform. This is not the case for the Galactic centre; however, we approximate it as so in order to make the problem tractable. It may seem especially bad for treatment of compact objects very close to the central MBH, inside the radius where main sequence stars would be tidally disrupted; however, it must be remembered that it is small angle deflections, rather than large deflections from close collisions, that are most important for relaxation. The error introduced by this assumption can be partially absorbed by the appropriate

choice of the Coloumb logarithm, which shall be introduced later (Just et al. 2011). Using an averaged value, the number of stars is

$$\mathrm{d}N = n(v_1,\theta,\varphi)\,\mathrm{d}v_1\,\mathrm{d}\theta\,\mathrm{d}\varphi\,\mathrm{d}^3r, \tag{A9}$$

using spherical polar coordinates for velocity space. Using D as the impact parameter for the encounter and Θ for the angle between the fundamental plane (containing $\boldsymbol{v}_1$ ans $\boldsymbol{v}_2$) and the the orbital plane, the number of events in time interval δt is

$$\mathrm{d}\Gamma = n(v_1,\theta,\varphi)\,\mathrm{d}v_1\,\mathrm{d}\theta\,\mathrm{d}\varphi\frac{\mathrm{d}\Theta}{2\pi}2\pi D\,\mathrm{d}DV\,\delta t. \tag{A10}$$

The squared change in energy for these encounters is

$$\Delta E^2(v_1,\theta,\varphi,D,\Theta) = (\Delta E)^2\,\mathrm{d}\Gamma \tag{A11}$$

$$= 4n(v_1,\theta,\varphi)V_\mathrm{g}^2V^3\left(\frac{m_1m_2}{m_1+m_2}\right)^2\cos^2 i\cos^2(\phi-\psi)\cos^2\psi D\,\mathrm{d}v_1\,\mathrm{d}\theta\,\mathrm{d}\varphi\,\mathrm{d}\Theta\,\mathrm{d}D\,\delta t. \tag{A12}$$

We must integrate out all these dependencies.

Since we have assumed that the stellar density does not depend upon position, we can simply integrate over the impact parameter; this is related to the deflection angle by

$$\frac{1}{\cos^2\psi} = 1 + \frac{D^2V^4}{G(m_1+m_2)}. \tag{A13}$$

Thus

$$\Delta E^2(v_1,\theta,\varphi,\psi,\Theta) = 4n(v_1,\theta,\varphi)\frac{V_\mathrm{g}^2}{V}G^2m_1^2m_2^2\cos^2 i\frac{\cos^2(\phi-\psi)\sin\psi}{\cos\psi}\,\mathrm{d}\psi\,\mathrm{d}v_1\,\mathrm{d}\theta\,\mathrm{d}\varphi\,\mathrm{d}\Theta\,\delta t. \tag{A14}$$

The integral over ψ is

$$I(\psi_0) = \int_0^{\psi_0}\frac{\cos^2(\phi-\psi)\sin\psi}{\cos\psi}\,\mathrm{d}\psi \tag{A15}$$

$$= \frac{\sin 2\phi}{2}\left(\psi_0 - \frac{\sin 2\psi_0}{2}\right) - \frac{\cos 2\phi}{2}\left(\frac{\cos 2\psi_0}{2}\right) - \sin^2\phi\ln(\cos\psi_0). \tag{A16}$$

Naively we would think that the upper limit for the deflection limit should be $\psi_0 = \pi/2$; however, this would introduce a logarithmic divergence. In actuality there is a physical cut-off, reflecting a finite bound for the maximum impact parameter D_0 (Weinberg 1986). This is set by the scale of the system, beyond which scattering is negligible. While the logarithmic term is finite, it is still large, dominating the other terms which are $\mathcal{O}(1)$; we therefore neglect the subdominant terms

$$\Delta E^2(v_1,\theta,\varphi,\Theta) \simeq 4n(v_1,\theta,\varphi)\frac{V_\mathrm{g}^2}{V}G^2m_1^2m_2^2\cos^2 i\sin^2\phi\ln\left(\frac{1}{\cos\psi_0}\right)\,\mathrm{d}v_1\,\mathrm{d}\theta\,\mathrm{d}\varphi\,\mathrm{d}\Theta\,\delta t. \tag{A17}$$

Next, we integrate over the orbital plane inclination using

$$\cos i\sin\phi = \sin\Phi\cos\Theta, \tag{A18}$$

so that

$$\Delta E^2(v_1,\theta,\varphi) \simeq 4\pi n(v_1,\theta,\varphi)\frac{V_\mathrm{g}^2}{V}G^2m_1^2m_2^2\sin^2\Phi\ln\left(\frac{1}{\cos\psi_0}\right)\,\mathrm{d}v_1\,\mathrm{d}\theta\,\mathrm{d}\varphi\,\delta t. \tag{A19}$$

We are now left with just the velocity variables.

An expression for $\sin^2\Phi$ can be obtained from (A1) and (A3), after some rearrangement

$$\frac{V_g^2}{V}\sin^2\Phi = \frac{v_1^2v_2^2\sin^2\theta}{(v_1^2+v_2^2-2v_1v_2\cos\theta)^{3/2}}. \tag{A20}$$

To proceed further we must specify the form of $n(v_1,\theta,\varphi)$, if we assume isotropy

$$n(v_1,\theta,\varphi) = n(v_1)\frac{1}{4\pi}\sin\theta. \tag{A21}$$

The integral over φ is then trivial,

$$\Delta E^2(v_1,\theta) \simeq \pi n(v_1)\frac{G^2m_1^2m_2^2v_1^2v_2^2\sin^3\theta}{(v_1^2+v_2^2-2v_1v_2\cos\theta)^{3/2}}\ln\left[1+\frac{D_0\left(v_1^2+v_2^2-2v_1v_2\cos\theta\right)^2}{G^2\left(m_1+m_2\right)^2}\right]\,\mathrm{d}v_1\,\mathrm{d}\theta\,\delta t. \tag{A22}$$

To integrate over θ it is easier to recast in terms of V; the integral is

$$J = v_1^2v_2^2\int_0^\pi\frac{\sin^3\theta}{(v_1^2+v_2^2-2v_1v_2\cos\theta)^{3/2}}\ln\left[1+\frac{D_0\left(v_1^2+v_2^2-2v_1v_2\cos\theta\right)^2}{G^2\left(m_1+m_2\right)^2}\right]\mathrm{d}\theta \tag{A23}$$

$$= v_1v_2\int_{V_-}^{V_+}\frac{\sin^2\theta}{V^2}\ln\left(1+q^2V^4\right)\mathrm{d}V, \tag{A24}$$

where the limits are

$$V_+ = v_1 + v_2; \quad V_- = |v_1 - v_2|, \tag{A25}$$

and we have introduced

$$q = \frac{D_0}{G\left(m_1 + m_2\right)}. \tag{A26}$$

Using (A3) to rearrange, and then integrating by parts gives

$$J = \frac{1}{4v_1v_2}\int_{V_-}^{V_+} \frac{\left(V_+^2 - V^2\right)\left(V^2 - V_-^2\right)}{V^2} \ln\left(1 + q^2V^4\right) \mathrm{d}V \tag{A27}$$

$$= \frac{1}{4v_1v_2}\left\{\left[\frac{3V_+^2V_-^2 + 3\left(V_+^2 + V_-^2\right)V^2 - V^4}{3V} \ln\left(1 + q^2V^4\right)\right]_{V_-}^{V_+} - \int_{V_-}^{V_+} \frac{3V_+^2V_-^2 + 3\left(V_+^2 + V_-^2\right)V^2 - V^4}{3V} \frac{4q^2V^3}{1 + q^2V^4} \mathrm{d}V\right\}; \tag{A28}$$

the former piece still contains the logarithmic term which we know must be large. It is therefore the dominant piece of the integral and we neglect the latter (Chandrasekhar 1941b),

$$J \simeq \frac{1}{6v_1v_2}\left[\left(3V_-^2 + V_+^2\right)V_+ \ln\left(1 + q^2V_+^4\right) - \left(3V_+^2 + V_-^2\right)V_- \ln\left(1 + q^2V_-^4\right)\right]. \tag{A29}$$

This may be further simplified, reusing the limit of large q (Chandrasekhar 1941b,c),

$$J \simeq \frac{1}{3v_1v_2}\left[\left(3V_-^2 + V_+^2\right)V_+ \ln\left(qV_+^2\right) - \left(3V_+^2 + V_-^2\right)V_- \ln\left(qV_-^2\right)\right] \tag{A30}$$

$$\simeq \frac{4}{3v_1v_2}\begin{cases}\left(v_1^3 + v_2^3\right)\ln\left[q\left(v_1 + v_2\right)^2\right] - \left(v_2^3 - v_1^3\right)\ln\left[q\left(v_1 - v_2\right)^2\right] & v_1 \leqslant v_2\\ \left(v_1^3 + v_2^3\right)\ln\left[q\left(v_1 + v_2\right)^2\right] - \left(v_1^3 - v_2^3\right)\ln\left[q\left(v_1 - v_2\right)^2\right] & v_1 \geqslant v_2\end{cases} \tag{A31}$$

$$\simeq \frac{8}{3}\begin{cases}\dfrac{v_2^2}{v_1}\ln\left(\dfrac{v_1 + v_2}{v_2 - v_1}\right) + \dfrac{v_1^2}{v_2}\left[\ln\left(qv_2^2\right) + \ln\left(1 - \dfrac{v_1^2}{v_2^2}\right)\right] & v_1 < v_2\\ v_2\left[\ln\left(qv_2^2\right) + \ln 4\right] & v_1 = v_2\\ \dfrac{v_1^2}{v_2}\ln\left(\dfrac{v_1 + v_2}{v_1 - v_2}\right) + \dfrac{v_2^2}{v_1}\left[\ln\left(qv_2^2\right) + \ln\left(\dfrac{v_1^2}{v_2^2} - 1\right)\right] & v_1 > v_2\end{cases} \tag{A32}$$

$$\approx \frac{8}{3}\begin{cases}\dfrac{v_1^2}{v_2}\ln\left(qv_2^2\right) & v_1 \leqslant v_2\\ \dfrac{v_2^2}{v_1}\ln\left(qv_2^2\right) & v_1 \geqslant v_2\end{cases}. \tag{A33}$$

This form maintains the correct limit for $v_2 \to 0$. We are left with

$$\Delta E^2(v_1) \simeq \frac{8\pi}{3}n(v_1)G^2m_1^2m_2^2\ln\left(qv_2^2\right)\left\{\begin{array}{ll}\dfrac{v_1^2}{v_2} & v_1 \leqslant v_2\\ \dfrac{v_2^2}{v_1} & v_1 \geqslant v_2\end{array}\right\}\mathrm{d}v_1\delta t. \tag{A34}$$

The final integral requires a specific form for the velocity distribution.

A2 Velocity distributions

The velocity space distribution function can be obtained by integrating out the spatial dependence in the full DF

$$f(v) = \int \mathrm{d}^3r f(\mathcal{E}). \tag{A35}$$

As we are restricting our attention to the Galactic centre and assuming spherical symmetry

$$f(v) = 4\pi\int_0^{r_c} r^2 f(\mathcal{E})\,\mathrm{d}r, \tag{A36}$$

where r_c is defined by (3). It is useful to work in terms of dimensionless variables

$$x = \frac{\mathcal{E}}{\sigma^2}; \tag{A37}$$

$$w = \frac{v^2}{2\sigma^2}. \tag{A38}$$

Changing the integral to be over dimensionless energy

$$f(v) = 4\pi r_c^3\int_\infty^{w-1} \frac{f(x)}{(w - x)^4}\,\mathrm{d}x, \tag{A39}$$

keeping w as a function of v.

The DF for unbound stars is assumed to be Maxwellian; it is defined in (5) and is applicable for $x > 0$, implying $w > 1$:

$$f_{\mathrm{u},\,M}(v) = \frac{N_*}{(2\pi\sigma^2)^{3/2}} C_M \int_0^{w-1} \frac{\exp(-x)}{(w-x)^4}\,\mathrm{d}x \tag{A40}$$

$$= \frac{N_*}{(2\pi\sigma^2)^{3/2}} C_M \epsilon\left(\frac{v^2}{2\sigma^2}\right), \tag{A41}$$

introducing

$$\epsilon(w) = \frac{1}{2}\left\{\exp(-w)\left[4\exp(1) + \mathrm{Ei}(w) - \mathrm{Ei}(1)\right] - \frac{2+w+w^2}{w^3}\right\}, \tag{A42}$$

where $\mathrm{Ei}(x)$ is the exponential integral.

The DF for bound stars is approximated as a simple power law as defined in (8), it is applicable for $x < 0$:

$$f_{\mathrm{b},\,M}(v) = \frac{N_*}{(2\pi\sigma^2)^{3/2}} k_M \begin{cases} \displaystyle\int_{-\infty}^{w-1} \frac{(-x)^{p_M}}{(w-x)^4}\,\mathrm{d}x & w \leqslant 1 \\ \displaystyle\int_{-\infty}^{0} \frac{(-x)^{p_M}}{(w-x)^4}\,\mathrm{d}x & w \geqslant 1 \end{cases}. \tag{A43}$$

The integral may be evaluated in terms of the hypergeometric function ${}_2F_1(a,b;c;x)$, but for the limits needed here the results simplify to

$$f_{\mathrm{b},\,M}(v) = \frac{N_*}{(2\pi\sigma^2)^{3/2}} k_M \left(\frac{v^2}{2\sigma^2}\right)^{p_M-3} \begin{cases} 3\,\mathrm{B}\left(\dfrac{v^2}{2\sigma^2}; 3-p_M, 1+p_M\right) & \dfrac{v^2}{2\sigma^2} \leqslant 1 \\ 3\,\mathrm{B}\left(3-p_M, 1+p_M\right) & \dfrac{v^2}{2\sigma^2} \geqslant 1 \end{cases}, \tag{A44}$$

where $\mathrm{B}(x;a,b)$ is the incomplete beta function (Olver et al. 2010, 8.17), $\mathrm{B}(a,b) \equiv \mathrm{B}(1,a,b)$ is the complete beta function.

The velocity space density is related to the distribution by

$$\frac{4\pi r_\mathrm{c}^3}{3} n_M(v_1) = 4\pi v_1^2 \left[f_{\mathrm{u},\,M}(v_1) + f_{\mathrm{b},\,M}(v_1)\right]. \tag{A45}$$

A3 Defining the relaxation time-scale

Using the specific forms for the velocity space density, we can calculate the squared change in energy. The functional form depends upon the velocity of the test star. If $v_2^2/2\sigma^2 < 1$, then

$$\begin{aligned}\Delta E^2 \simeq \frac{8}{3}\sqrt{2\pi}\frac{G^2 m_1^2 m_2^2 n_*}{\sigma^3}\ln\left(qv_2^2\right)\Bigg\{&\int_0^{v_2} 3k\frac{v_1^4}{v_2}\left(\frac{v_1^2}{2\sigma^2}\right)^{p-3}\mathrm{B}\left(\frac{v_1^2}{2\sigma^2}; 3-p, 1+p\right)\mathrm{d}v_1 \\ &+ \int_{v_2}^{\sqrt{2}\sigma} 3kv_1v_2^2\left(\frac{v_1^2}{2\sigma^2}\right)^{p-3}\mathrm{B}\left(\frac{v_1^2}{2\sigma^2}; 3-p, 1+p\right)\mathrm{d}v_1 \\ &+ \int_{\sqrt{2}\sigma}^{\infty} v_1v_2^2\left[3k\left(\frac{v_1^2}{2\sigma^2}\right)^{p-3}\mathrm{B}\left(3-p_M, 1+p_M\right) + C\epsilon\left(\frac{v_1^2}{2\sigma^2}\right)\right]\mathrm{d}v_1\Bigg\}\,\delta t,\end{aligned} \tag{A46}$$

where we have suppressed the subscript M for brevity; it would be necessary to sum over all the species to get the total value. Computing the integrals and rearranging yields

$$\Delta E^2 \simeq \frac{16}{3}\sqrt{2\pi}\frac{G^2 m_1^2 m_2^2 n_*}{\sigma^3}\ln\left(qv_2^2\right)\left(\frac{v_2^2}{2\sigma^2}\right)\left[k\frac{3}{(2-p)(1+p)}{}_3F_2\left(-1-p, 2-p, \frac{3}{2}; 3-p, \frac{5}{2}; \frac{v_2^2}{2\sigma^2}\right) + C\right]\delta t, \tag{A47}$$

where ${}_3F_2(a_1,a_2,a_3;b_1,b_2;x)$ is a generalised hypergeometric function (Olver et al. 2010, section 16). The contribution from bound and unbound stars can be identified by the coefficients k and C respectively.

If $v_2^2/2\sigma^2 > 1$,

$$\begin{aligned}\Delta E^2 \simeq \frac{8}{3}\sqrt{2\pi}\frac{G^2 m_1^2 m_2^2 n_*}{\sigma^3}\ln\left(qv_2^2\right)\Bigg\{&\int_0^{\sqrt{2}\sigma} 3k\frac{v_1^4}{v_2}\left(\frac{v_1^2}{2\sigma^2}\right)^{p-3}\mathrm{B}\left(\frac{v_1^2}{2\sigma^2}; 3-p, 1+p\right)\mathrm{d}v_1 \\ &+ \int_{\sqrt{2}\sigma}^{v_2} \frac{v_1^4}{v_2}\left[3k\left(\frac{v_1^2}{2\sigma^2}\right)^{p-3}\mathrm{B}\left(3-p, 1+p\right) + C\epsilon\left(\frac{v_1^2}{2\sigma^2}\right)\right]\mathrm{d}v_1 \\ &+ \int_{v_2}^{\infty} v_1v_2^2\left[3k\left(\frac{v_1^2}{2\sigma^2}\right)^{p-3}\mathrm{B}\left(3-p_M, 1+p_M\right) + C\epsilon\left(\frac{v_1^2}{2\sigma^2}\right)\right]\mathrm{d}v_1\Bigg\}\,\delta t.\end{aligned} \tag{A48}$$

Computing this gives

$$\Delta E^2 \simeq \frac{16}{3}\sqrt{2\pi}G^2 m_1^2 m_2^2 n_* \sigma \ln\left(q v_2^2\right)\left(\frac{v_2^2}{2\sigma^2}\right)^{-1/2}\left[k\beta\left(\frac{v_2^2}{2\sigma^2};p\right)+C\alpha\left(\frac{v_2^2}{2\sigma^2}\right)\right]\delta t, \tag{A49}$$

where

$$\begin{aligned}\alpha(w) = \frac{1}{2}\Bigg\{&3w^{-1/2}+5+\left[4\exp(1)-\mathrm{Ei}(1)+\mathrm{Ei}(w)\right]\left[\frac{3\sqrt{\pi}}{4}\,\mathrm{erf}\left(w^{1/2}\right)-\frac{3}{2}w^{1/2}\exp(-w)\right]-3\sqrt{\pi}\exp(1)\,\mathrm{erf}(1)\\ &+3\left[{}_2F_2\left(\frac{1}{2},1;\frac{3}{2},\frac{3}{2};1\right)-w^{1/2}{}_2F_2\left(\frac{1}{2},1;\frac{3}{2},\frac{3}{2};w\right)\right]\Bigg\};\end{aligned} \tag{A50}$$

$$\beta(w;p) = \begin{cases}\dfrac{3}{1/2-p}\left[\mathrm{B}\left(\dfrac{5}{2},1+p\right)-\dfrac{3w^{p-1/2}}{2(2-p)}\,\mathrm{B}\left(3-p,1+p\right)\right] & p<\dfrac{1}{2}\\ \dfrac{\pi}{32}\left[12\ln(2)-1+6\ln(w)\right] & p=\dfrac{1}{2}\end{cases}. \tag{A51}$$

The generalised hypergeometric function originates from the integral

$$\int^w \frac{\exp(w')\,\mathrm{erf}\left(w'^{1/2}\right)}{w'}\,\mathrm{d}w' = \frac{4w^{1/2}}{\sqrt{\pi}}{}_2F_2\left(\frac{1}{2},1;\frac{3}{2},\frac{3}{2};w\right). \tag{A52}$$

Combining the two regimes gives some quite complicated expressions. It is possible to simplify these while maintaining reasonable accuracy, for this purpose we separate the contributions from bound and unbound stars. The bound contribution is relatively straightforward for larger v_2; for smaller v_2 we may use a series expansion in $v_2^2/2\sigma^2 < 1$ to approximate the hypergeometric function:

$$\Delta E_{\mathrm{b}}^2 \approx \frac{16}{3}\sqrt{2\pi}G^2 m_1^2 m_2^2 n_* \sigma \ln\left(q v_2^2\right) k \left\{\begin{array}{ll}\dfrac{3}{(1+p)(2-p)}\left(\dfrac{v_2^2}{2\sigma^2}\right)-\dfrac{9}{5(3-p)}\left(\dfrac{v_2^2}{2\sigma^2}\right)^2+\dfrac{9p}{14(7-p)}\left(\dfrac{v_2^2}{2\sigma^2}\right)^3 & \dfrac{v_2^2}{2\sigma^2}<1\\ \left(\dfrac{v_2^2}{2\sigma^2}\right)^{-1/2}\beta\left(\dfrac{v_2^2}{2\sigma^2};p\right) & \dfrac{v_2^2}{2\sigma^2}>1\end{array}\right\}\delta t. \tag{A53}$$

This can be rolled into one continuous function

$$\begin{aligned}\Delta E_{\mathrm{b}}^2 &\approx \frac{16}{3}\sqrt{2\pi}G^2 m_1^2 m_2^2 n_* \sigma \ln\left(q v_2^2\right) k\left[1+\left(\frac{v_2^2}{2\sigma^2}\right)^4\right]^{-1}\Bigg\{\left[\frac{3}{(1+p)(2-p)}\left(\frac{v_2^2}{2\sigma^2}\right)-\frac{9}{5(3-p)}\left(\frac{v_2^2}{2\sigma^2}\right)^2+\frac{9p}{14(7-p)}\left(\frac{v_2^2}{2\sigma^2}\right)^3\right]\\ &\quad+\left(\frac{v_2^2}{2\sigma^2}\right)^{7/2}\beta\left(\frac{v_2^2}{2\sigma^2};p\right)\Bigg\}\delta t \qquad\qquad (A54)\\ &\approx 16\sqrt{2\pi}G^2 m_1^2 m_2^2 n_* \sigma \ln\left(q v_2^2\right) k\gamma\left(\frac{v_2^2}{2\sigma^2};p\right)\delta t, \qquad\qquad (A55)\end{aligned}$$

defining the function $\gamma(w;p)$ in the last line. The resulting error [ignoring variation from $\ln\left(qv_2^2\right)$] is less than 3%.

The unbound contribution is very simple for small v_2, but much more complicated for large v_2. In the limit of $v_2 \to \infty$, it decays as v_2^{-1}:

$$\begin{aligned}\lim_{w\to\infty}\{\alpha(w)\} &= \frac{1}{2}\left\{5+3\sqrt{\pi}\left[\exp(1)-\frac{\mathrm{Ei}(1)}{4}-\exp(1)\,\mathrm{erf}(1)\right]+3{}_2F_2\left(\frac{1}{2},1;\frac{3}{2},\frac{3}{2};1\right)\right\} &(A56)\\ &= \Xi \simeq 4.31. &(A57)\end{aligned}$$

Using the two limiting forms, the function

$$\Delta E_{\mathrm{u}}^2 \approx \frac{16}{3}\sqrt{2\pi}G^2 m_1^2 m_2^2 n_* \sigma \ln\left(q v_2^2\right) C\Xi\left(\frac{v_2^2}{2\sigma^2}\right)\left[\Xi^2+\left(\frac{v_2^2}{2\sigma^2}\right)^3\right]^{-1/2}\delta t, \tag{A58}$$

reproduces the full function to better than 5% [ignoring variation from $\ln\left(qv_2^2\right)$].

Making explicit the sum over the different species, the total change in energy squared is approximately

$$\Delta E^2 \approx \sum_M \frac{16}{3}\sqrt{2\pi}G^2 M^2 m_2^2 n_* \sigma \ln\left(q v_2^2\right)\left\{k_M\gamma\left(\frac{v_2^2}{2\sigma^2};p_M\right)+C_M\Xi\left(\frac{v_2^2}{2\sigma^2}\right)\left[\Xi^2+\left(\frac{v_2^2}{2\sigma^2}\right)^3\right]^{-1/2}\right\}\delta t. \tag{A59}$$

The relaxation time-scale is the time interval δt over which the squared change in energy becomes equal to the kinetic energy

of the test star squared (Bar-Or et al. 2012)

$$\tau_{\mathrm{R}} = \left(\frac{m_2 v_2^2}{2}\right)^2 \frac{\delta t}{\Delta E^2} \tag{A60}$$

$$\approx \frac{3v_2^4}{16\sqrt{2\pi}G^2 n_* \sigma \ln\left(q v_2^2\right)} \left(\sum_M M^2 \left\{ k_M \gamma\left(\frac{v_2^2}{2\sigma^2}; p_M\right) + C_M \Xi\left(\frac{v_2^2}{2\sigma^2}\right)\left[\Xi^2 + \left(\frac{v_2^2}{2\sigma^2}\right)^3\right]^{-1/2} \right\}\right)^{-1}. \tag{A61}$$

This is the time required for stellar encounters to become effective in changing the energy of an orbit in the smooth background potential. The use of the squared change in energy reflects the expectation that energy changes like a random walk, and hence scales with the square-root of the time.

A4 Averaged time-scale

The relaxation time-scale defined above is appropriate for a particular initial test star velocity v_2. This is not of much use to describe the Galactic centre or even a (non-circular) orbit where there is a range in velocity. It is necessary to calculate an averaged time-scale. Both the change in energy squared and the kinetic energy are averaged; comparing these gives the appropriate time-scale. We shall use two averages: over the distribution of bound velocities to give the relaxation time-scale for the system, and over a single orbit. The former shall be of use when considering the inner cut-off of stars due to collisions, the latter when considering the transition to gravitational wave inspiral.

A4.1 System relaxation time-scale

The total number of bound stars in the core is

$$N_{\mathrm{b},\,M} = \frac{3}{3/2 - p_M} \frac{\Gamma(p_M + 1)}{\Gamma(p_M + 7/2)} N_* k_M, \tag{A62}$$

where $\Gamma(x)$ is the gamma function. Using this as a normalisation constant, the probability of a bound star having a velocity in the range $v \to v + \mathrm{d}v$ is given by

$$4\pi v^2 p_{\mathrm{b},\,M}(v)\,\mathrm{d}v = 4\pi v^2 \frac{f_{\mathrm{b},\,M}(v)}{N_{\mathrm{b},\,M}}\,\mathrm{d}v \tag{A63}$$

$$= \sqrt{\frac{2}{\pi}} \frac{v^2}{\sigma^3} \frac{(3/2 - p_M)\,\Gamma(p_M + 7/2)}{\Gamma(p_M + 1)} \left(\frac{v^2}{2\sigma^2}\right)^{p_M - 3} \left\{ \begin{array}{ll} \mathrm{B}\left(\dfrac{v^2}{2\sigma^2}; 3 - p_M, 1 + p_M\right) & \dfrac{v^2}{2\sigma^2} \leqslant 1 \\ \mathrm{B}\left(3 - p_M, 1 + p_M\right) & \dfrac{v^2}{2\sigma^2} \geqslant 1 \end{array} \right\} \mathrm{d}v. \tag{A64}$$

The mean squared velocity for bound stars in the core is then

$$\overline{v_M^2} = 4\pi \int_0^\infty v^4 p_{\mathrm{b},\,M}(v)\,\mathrm{d}v \tag{A65}$$

$$= 3\sigma^2 \frac{3/2 - p_M}{1/2 - p_M}, \tag{A66}$$

assuming that $p_M < 1/2$.

In the case $p_M = 1/2$ the integral no longer converges, we encounter a logarithmic divergence. This is not a concern, just as with the divergence encountered in Sec. A1, it reflects there being a physical cut-off; in this case there is a maximal velocity. We use $v_{\max} = c/2$, which is the maximum speed reached on a bound orbit about a Schwarzschild BH. Marginally higher speeds can be reached for prograde orbits about a Kerr BH, but the maximal velocity for retrograde orbits is marginally lower. In reality, we might expect the maximum velocity to be lower due to a depletion of orbits (for example because of gravitational wave inspiral). We neglect these possible variations, since the error introduced should be small as a consequence of taking the logarithm. We also suspect that a simple Newtonian description of these orbits is imprecise, but a full relativistic description is beyond this simple analysis. For $p_M = 1/2$,

$$\overline{v_M^2} = \frac{\sigma^2}{2}\left[12\ln(2) - 5 + 6\ln\left(\frac{v_{\max}^2}{2\sigma^2}\right)\right]. \tag{A67}$$

Using a typical value of $\sigma = 10^5\ \mathrm{m\,s^{-1}}$,

$$\overline{v_M^2} \simeq 43\sigma^2. \tag{A68}$$

The mean squared velocity is an order of magnitude greater than for a Maxwellian distribution.

The average of the change in energy is more involved. First we replace the term $\ln\left(q v_2^2\right)$ in ΔE^2 by a suitable average so that it may be moved outside the integral (Chandrasekhar 1960, chapter 2). We assume that it may be replaced by the Coulomb logarithm, which can be approximated as (Bahcall & Wolf 1976)

$$\ln\left(q\overline{v_2^2}\right) = \ln\Lambda_M \simeq \ln\left(\frac{M_\bullet}{M}\right). \tag{A69}$$

Just et al. (2011) find an extremely similar result fitting a Bahcall–Wolf cusp self-consistently. We calculate the averages for the bound and unbound contributions individually. In calculating the bound component we must distinguish between the the bound population of field stars and the distribution of test stars over which we are averaging. We use M and M' respectively as subscripts for this calculation.[9] The average is

$$\overline{\Delta E^2_{\mathrm{b},\,M'}} = 4\pi \int_0^\infty \Delta E^2_{\mathrm{b}} v^2 p_{\mathrm{b},\,M'}(v)\,\mathrm{d}v \tag{A70}$$

$$\begin{aligned} &\simeq \sum_M \frac{32}{3}\frac{G^2M^2M'^2 n_*}{\sigma^2}\ln\left(\Lambda_{M'}\right) k_M \frac{(3/2-p_{M'})\Gamma(p_{M'}+7/2)}{\Gamma(p_{M'}+1)} \\ &\quad\times\left[\int_0^{\sqrt{2}\sigma} v^2\left(\frac{v^2}{2\sigma^2}\right)^{p_{M'}-2}\frac{3}{(2-p_M)(1+p_M)}{}_3F_2\left(-1-p_M,2-p_M,\frac{3}{2};3-p_M,\frac{5}{2};\frac{v^2}{2\sigma^2}\right)\mathrm{B}\left(\frac{v^2}{2\sigma^2};3-p_{M'},1+p_{M'}\right)\mathrm{d}v\right. \\ &\quad\left.+\int_{\sqrt{2}\sigma}^\infty v^2\left(\frac{v^2}{2\sigma^2}\right)^{p_{M'}-7/2}\beta\left(\frac{v^2}{2\sigma^2};p_M\right)\mathrm{B}\left(3-p_M,1+p_M\right)\mathrm{d}v\right]\delta t. \end{aligned} \tag{A71}$$

The high velocity integral can be performed without difficulty, but the low velocity piece is more formidable. Progress can be made by making a series expansion in $v^2/2\sigma^2$. Retaining terms to third order approximates the integrand to no worse than 10%, with good agreement across most of the integration range. The result may be condensed into a simpler form by approximating it as a quadratic in p_M and $p_{M'}$, which introduces less than 2% further error. After this manipulation

$$\begin{aligned} \overline{\Delta E^2_{\mathrm{b},\,M'}} \approx \sum_M \frac{2^{11/2}}{3}G^2M^2M'^2 n_*\sigma\ln\left(\Lambda_{M'}\right)k_M\frac{(3/2-p_{M'})\Gamma(p_{M'}+7/2)}{\Gamma(p_{M'}+1)}\left\{\frac{1}{210}\left[30+36p_M+25p_M^2-p_{M'}\left(13+15p_M+7p_M^2\right)\right.\right. \\ \left.\left.+\;p_{M'}^2\left(6+9p_M+8p_M^2\right)\right]+\iota\left(p_M,p_{M'}\right)\right\}\delta t, \end{aligned} \tag{A72}$$

introducing

$$\iota\left(p_M,p_{M'}\right)=\mathrm{B}\left(3-p_{M'},1+p_{M'}\right)\begin{cases}\dfrac{3}{1/2-p_M}\left[\dfrac{\mathrm{B}\left(5/2,1+p_M\right)}{2-p_{M'}}-\dfrac{3\,\mathrm{B}\left(3-p_M,1+p_M\right)}{2\left(2-p_M\right)\left(5/2-p_M-p_{M'}\right)}\right] & p_M<\dfrac{1}{2}\\ \dfrac{\pi}{32}\dfrac{4+p_{M'}+12\left(2-p_{M'}\right)\ln(2)}{\left(2-p_{M'}\right)^2} & p_M=\dfrac{1}{2}\end{cases}. \tag{A73}$$

To calculate the unbound component we use the exact form for the low velocity component and the approximate form of (A58).

$$\overline{\Delta E^2_{\mathrm{u},\,M'}} = 4\pi \int_0^\infty \Delta E^2_{\mathrm{u}} v^2 p_{\mathrm{b},\,M'}(v)\,\mathrm{d}v \tag{A74}$$

$$\begin{aligned} &\approx \sum_M \frac{32}{3}\frac{G^2M^2M'^2 n_*}{\sigma^2}\ln\left(\Lambda_{M'}\right) C_M \frac{(3/2-p_{M'})\Gamma(p_{M'}+7/2)}{\Gamma(p_{M'}+1)}\left\{\int_0^{\sqrt{2}\sigma} v^2\left(\frac{v^2}{2\sigma^2}\right)^{p_{M'}-2}\mathrm{B}\left(\frac{v^2}{2\sigma^2};3-p_{M'},1+p_{M'}\right)\mathrm{d}v\right. \\ &\quad\left.+\int_{\sqrt{2}\sigma}^\infty v^2\left(\frac{v^2}{2\sigma^2}\right)^{p_{M'}-2}\Xi\left[\Xi^2+\left(\frac{v^2}{2\sigma^2}\right)^3\right]^{-1/2}\mathrm{B}\left(3-p_M,1+p_M\right)\mathrm{d}v\right\}\delta t; \end{aligned} \tag{A75}$$

for consistency with the bound case we have continued to use the subscript M'. The low velocity integral is of the same form as for calculating $\overline{v^2_M}$ and can be evaluated in terms of beta functions, the high velocity integral can be evaluated in terms of the hypergeometric function (Olver et al. 2010, 15.6.1)

$$\begin{aligned} \overline{\Delta E^2_{\mathrm{u},\,M'}} \approx \sum_M \frac{2^{11/2}}{3}G^2M^2M'^2 n_*\sigma\ln\left(\Lambda_{M'}\right)C_M\frac{(3/2-p_{M'})\Gamma(p_{M'}+7/2)}{\Gamma(p_{M'}+1)} \\ \times\left[\nu\left(p_{M'}\right)+\Xi\frac{\mathrm{B}\left(3-p_{M'},1+p_{M'}\right)}{2-p_{M'}}{}_2F_1\left(\frac{1}{2},\frac{2-p_{M'}}{3};\frac{5-p_{M'}}{3};-\Xi^2\right)\right]\delta t, \end{aligned} \tag{A76}$$

where

$$\nu(p)=\begin{cases}\dfrac{1}{1/2-p}\left[\mathrm{B}\left(\dfrac{5}{2},1+p\right)-\mathrm{B}\left(3-p,1+p\right)\right] & p<\dfrac{1}{2}\\ \dfrac{\pi}{96}\left[12\ln(2)-5\right] & p=\dfrac{1}{2}\end{cases}. \tag{A77}$$

[9] For masses: $m_M \equiv M$, $m_{M'} \equiv M'$.

The total relaxation time for a species is

$$\overline{\tau_{\mathrm{R},\,M'}} = \left(\frac{M'\overline{v_{M'}^2}}{2}\right)^2 \frac{\delta t}{\overline{\Delta E_{\mathrm{b},\,M'}^2} + \overline{\Delta E_{\mathrm{u},\,M'}^2}} \tag{A78}$$

$$\begin{aligned} &\approx \frac{3}{2^{15/2}} \frac{\Gamma(p_{M'}+1)}{(3/2-p_{M'})\Gamma(p_{M'}+7/2)} \frac{\overline{v_{M'}^2}^2}{G^2 n_* \sigma \ln(\Lambda_{M'})} \\ &\quad \times \left\{ \sum_M k_M M^2 \left[\frac{30 + 36p_M + 25p_M^2 - p_{M'}\left(13 + 15p_M + 7p_M^2\right) + p_{M'}^2\left(6 + 9p_M + 8p_M^2\right)}{210} + \iota\left(p_M, p_{M'}\right) \right] \right. \\ &\quad \left. + C_M M^2 \left[\nu\left(p_{M'}\right) + \Xi \frac{\mathrm{B}\left(3 - p_{M'}, 1 + p_{M'}\right)}{2 - p_{M'}} {}_2F_1\left(\frac{1}{2}, \frac{2-p_{M'}}{3}; \frac{5-p_{M'}}{3}; -\Xi^2\right) \right] \right\}^{-1}. \end{aligned} \tag{A79}$$

Combining these to form an average for the entire system gives

$$\overline{\tau_{\mathrm{R}}} = \frac{\sum_{M'} N_{\mathrm{b},\,M'} \overline{\tau_{\mathrm{R},\,M'}}}{\sum_M N_{\mathrm{b},\,M}}. \tag{A80}$$

The relaxation time-scale for individual components is used in determining the collisional cut-off as described in Sec. 3.4.4.

A4.2 Orbital average

Defining a relaxation time-scale for an individual orbit gives an indication of how important two-body interactions are for the evolution of the orbit. It is useful for comparison with other time-scales to determine which process is dominant. We calculate the time-scale for an orbit, parameterised by e and r_{p}, by averaging over one period.[10] Two-body scattering will mean that a star shall not remain on the same orbit for an entire period. The time-scale is an estimate of the average rate of change in energy for stars instantaneously following that orbit. If the time-scale is much longer than the orbital period it is safe to assume that dynamical friction plays a small role over an orbit and to approximate the orbital elements as constant over the orbit. If the time-scale is much shorter than the period we expect that a star would be scattered from that orbit before it has chance to complete a cycle.

As for the system relaxation time-scale, we calculate the orbital time-scale by averaging the velocity squared and the squared change in energy. The mean squared velocity is [cf. (10)]

$$\left\langle v^2\left(e, r_{\mathrm{p}}\right)\right\rangle = \frac{GM_\bullet(1-e)}{r_{\mathrm{p}}}. \tag{A81}$$

The orbital average is calculated according to (Spitzer 1987, section 2.2b)

$$\langle X \rangle = \frac{1}{T}\int_0^T X(t)\,\mathrm{d}t, \tag{A82}$$

where T is the orbital period

$$T = 2\pi\sqrt{\frac{r_{\mathrm{p}}^3}{GM_\bullet(1-e)^3}}. \tag{A83}$$

This can be rewritten as

$$\langle X \rangle = \frac{2}{T}\int_0^\pi \frac{X(\vartheta)}{\dot{\vartheta}}\,\mathrm{d}\vartheta \tag{A84}$$

with orbital phase angle ϑ; here

$$\dot{\vartheta} = \sqrt{\frac{GM_\bullet}{r_{\mathrm{p}}^3(1+e)^3}}(1 + e\cos\vartheta)^2. \tag{A85}$$

In terms of the orbital phase, the velocity is

$$v(\vartheta) = \sqrt{\frac{GM_\bullet}{r_{\mathrm{p}}(1+e)}\left(1 + e^2 + 2e\cos\vartheta\right)}. \tag{A86}$$

[10] We only consider bound orbits. The orbital relaxation time-scale will be compared against the gravitational wave time-scale. We argue that the evolution of unbound orbits due to gravitational wave emission is negligible, so we do not need a relaxation time-scale for unbound orbits.

Substituting in the approximate expressions for the squared change in energy, (A55) and (A58),

$$\left\langle \Delta E^2_{\mathrm{b},\,M'} \right\rangle = \frac{\left(1-e^2\right)^{3/2}}{\pi} \int_0^\pi \frac{\Delta E^2_{\mathrm{b},\,M'}}{(1+e\cos\vartheta)^2}\,\mathrm{d}\vartheta \tag{A87}$$

$$\approx \sum_M \frac{16}{3}\sqrt{\frac{2}{\pi}} G^2 M^2 M'^2 n_* \sigma \left(1-e^2\right)^{3/2} \ln\left(\Lambda_{M'}\right) k_M \times \int_0^\pi \frac{1}{(1+e\cos\vartheta)^2} \gamma\left(\frac{r_\mathrm{c}}{2(1+e)r_\mathrm{p}}\left(1+e^2+2e\cos\vartheta\right); p_M\right)\mathrm{d}\vartheta\,\delta t, \tag{A88}$$

and

$$\left\langle \Delta E^2_{\mathrm{u},\,M'} \right\rangle = \frac{\left(1-e^2\right)^{3/2}}{\pi} \int_0^\pi \frac{\Delta E^2_{\mathrm{u},\,M'}}{(1+e\cos\vartheta)^2}\,\mathrm{d}\vartheta \tag{A89}$$

$$\approx \sum_M \frac{16}{3}\sqrt{\frac{2}{\pi}} G^2 M^2 M'^2 n_* \sigma \left(1-e^2\right)^{3/2} \ln\left(\Lambda_{M'}\right) C_M \times \int_0^\pi \frac{\Xi}{(1+e\cos\vartheta)^2}\left[\frac{r_\mathrm{c}}{2(1+e)r_\mathrm{p}}\left(1+e^2+2e\cos\vartheta\right)\right]\left\{\Xi^2+\left[\frac{r_\mathrm{c}}{2(1+e)r_\mathrm{p}}\left(1+e^2+2e\cos\vartheta\right)\right]^3\right\}^{-1/2}\mathrm{d}\vartheta\,\delta t. \tag{A90}$$

Despite our best efforts, we have been unsuccessful at obtaining analytic forms for these two integrals, and therefore compute them numerically. We define

$$I_\mathrm{b}(e,\varrho,p) = \int_0^\pi \frac{1}{(1+e\cos\vartheta)^2}\gamma\left(\frac{1}{2(1+e)\rho}\left(1+e^2+2e\cos\vartheta\right); p\right)\mathrm{d}\vartheta \tag{A91}$$

$$I_\mathrm{u}(e,\varrho,\Xi) = \int_0^\pi \frac{\Xi}{(1+e\cos\vartheta)^2}\left[\frac{1}{2(1+e)\rho}\left(1+e^2+2e\cos\vartheta\right)\right]\left\{\Xi^2+\left[\frac{1}{2(1+e)\rho}\left(1+e^2+2e\cos\vartheta\right)\right]^3\right\}^{-1/2}\mathrm{d}\vartheta. \tag{A92}$$

The orbital relaxation time-scale is then

$$\left\langle \tau_{\mathrm{R},\,M'}\left(e,r_\mathrm{p}\right)\right\rangle = \left(\frac{GM_\bullet(1-e)M'}{2r_\mathrm{p}}\right)^2 \frac{\delta t}{\left\langle \Delta E^2_{\mathrm{b},\,M'}\right\rangle + \left\langle \Delta E^2_{\mathrm{u},\,M'}\right\rangle} \tag{A93}$$

$$\approx \frac{3}{64}\sqrt{\frac{\pi}{2}}\frac{M_\bullet^2(1-e)^{1/2}}{n_*\sigma r_\mathrm{p}^2(1+e)^{3/2}\ln\left(\Lambda_{M'}\right)}\left[\sum_M k_M M^2 I_\mathrm{b}\left(e,\frac{r_\mathrm{p}}{r_\mathrm{c}},p_M\right) + C_M M^2 I_\mathrm{u}\left(e,\frac{r_\mathrm{p}}{r_\mathrm{c}},\Xi\right)\right]^{-1}. \tag{A94}$$

This time-scale is defined similarly to the inspiral time-scale (34).

Diffusion in angular momentum proceeds over a shorter time, as defined by (33). Combining this with (A94) gives the orbital angular momentum relaxation time-scale. Comparing this to the inspiral time-scale τ_GW can therefore determine whether gravitational wave inspiral or scattering takes place over a shorter time-scale, and so if we may expect an orbit, on average, to be depopulated as described in Sec. 3.4.3.

A5 Discussion of applicability

In deriving the relaxation time-scales it has been necessary to make a number of approximations, both mathematical and physical. The mathematical approximations have been to simplify functional forms and make the computations easier. We have been careful to ensure that the inaccuracies introduced are of the order of a few percent, and thus should be subdominant to the errors inherent from the physical assumptions and uncertainties in astronomical quantities. The physical approximations are more important. There are two key approximations that may limit the validity of the results.

First, it was assumed that the density of stars was uniform. This was a pragmatic assumption necessary to perform integrals over impact parameter and angular orientation. It is certainly not the case that density in the Galactic centre is uniform. However, this approximation is not as bad as it first may seem. As a star travels about the MBH on its orbit it moves through regions of different densities. It therefore samples a range of different density-impact parameter distributions. At a given radius stars will be travelling in a variety of directions meaning that again there will be a selection of different density-impact parameter distributions. Since we are only concerned with averaged time-scales, we may hope that this is sufficient to partially smear out changes in the density (cf. Just et al. 2011). To incorporate the complexity of the proper density distribution would require numerical evaluation of the distribution, and then numerical computation of the integrals. This would greatly obfuscate the analysis.

Second, we have only considered transfer of energy; transfer of angular momentum could be more important because of resonant relaxation which enhances angular momentum (both scalar and vector) diffusion (Rauch & Tremaine 1996; Rauch & Ingalls 1998; Gürkan & Hopman 2007; Eilon et al. 2009). This occurs in systems where the radial and azimuthal frequencies are commensurate. Orbits precess slowly leading to large torques between the orbits. These torques cause the

angular momentum to change linearly with time over a coherence time-scale set by the drift in orbits. Over longer time periods, the change in angular momentum again proceeds as a random walk, increasing with the square-root of time, as for non-resonant relaxation; however, it is still enhanced because of the change in the basic step size.

Resonant relaxation is important in systems with (nearly) Keplerian potentials, but is quenched when relativistic precession becomes significant: inside the Schwarzschild barrier (Merritt et al. 2011). It is therefore less likely to be of concern for the orbits significantly influenced by gravitational wave emission (Sigurdsson & Rees 1997).

For resonant relaxation, diffusion of energy remains unchanged; there could be several orders of magnitude difference in the two relaxation time-scales. While the enhanced angular momentum diffusion is of significance to the evolution of the system, the energy relaxation time-scale should still be relevant. It sets the time-scale for non-resonant relaxation [see (31)], and defines the time for the system to reach a steady-state, since diffusion of energy is the limiting process.

We have still considered the role played by angular momentum diffusion, assuming non-resonant relaxation, by defining the angular momentum relaxation time-scale $\tau_{\mathcal{J}}$ in Sec. 3.4.3 from the energy relaxation time-scale. This should be sufficient for our level of accuracy.

The optimal resolution would to be to perform a full N-body simulation of the Galactic centre. This would dispense with all the complications of considering relaxation time-scales and estimates for cut-off radii. Unfortunately such a task still remains computationally challenging at the present time [see, for example Li et al. (2012)].

A6 Time-scales for the Galactic centre

Evaluating the formulae for average relaxation time-scales with values appropriate for the Galactic centre (Sec. 3.2) provides some insight. Comparison of the system relaxation time-scales with that evaluated using a Maxwellian distribution (30), using $\kappa = 0.34$, shows a broad consistency:

$$\overline{\tau_{\mathrm{R}}} \simeq 2.0\tau_{\mathrm{R}}^{\mathrm{Max}}. \tag{A95}$$

This is reassuring since the standard Maxwellian approximation has been successful in characterising the properties of the Galactic centre. We have calculated the Maxwellian time-scale for the dominant stellar component alone, which gives $\tau_{\mathrm{R}}^{\mathrm{Max}} \simeq 4.5 \times 10^9$ yr.

If we look at the time-scales for each species in turn:

$$\overline{\tau_{\mathrm{R,\,MS}}} \simeq 1.7\tau_{\mathrm{R}}^{\mathrm{Max}}; \quad \overline{\tau_{\mathrm{R,\,WD}}} \simeq 1.6\tau_{\mathrm{R}}^{\mathrm{Max}}; \quad \overline{\tau_{\mathrm{R,\,NS}}} \simeq 2.1\tau_{\mathrm{R}}^{\mathrm{Max}}. \tag{A96}$$

Again there is good agreement.[11] For black holes,

$$\overline{\tau_{\mathrm{R,\,BH}}} \simeq 48\tau_{\mathrm{R}}^{\mathrm{Max}}. \tag{A97}$$

This time-scale is much larger on account of the higher mean-squared velocity.

The time-scales for the lighter components are of the order of the Hubble time. The BH time-scale is much longer. This may indicate that the BH population is not fully relaxed: we may expect that there has not been sufficient time for objects to diffuse onto the most tightly bound orbits. If this were the case, the mean-squared velocity of the population would be lower. In reality, we may expect that many of the most tightly bound BHs are not in a relaxed state, since gravitational wave inspiral will be the dominant effect in determining the profile. This would deplete some of the inner-most orbits, and should lower the mean square velocity for the population.

The long BH time-scale also inevitably includes an artifact of our approximation that the system is homogeneous: in reality the BHs, being more tightly clustered towards the centre, will pass through regions with greater density (both because of higher number density and a greater average object mass). Therefore, we may expect the true relaxation time-scale to be reduced.

Formation of the cusp can occur over shorter time than the relaxation time-scale (Bar-Or et al. 2012). It should proceed on a dynamical friction time-scale; this is shorter than the relaxation time-scale by a factor $\tau_{\mathrm{DF}} \approx (M_\star/M')\overline{\tau_{\mathrm{R},\,M'}}$ (Spitzer 1987, section 3.4). This does reduce the difference between the different species, but does not make it obvious that the cusp will have had sufficient time to form, especially if there has been a major merger in the Galaxy's history which would have disrupted the central distribution of stars (Gualandris & Merritt 2012). Fortunately, observations of the thick disc indicate that there has not been a major merger in the last 10^{10} yr (Wyse 2008).

The existence of a cusp is a subject of debate. Preto & Amaro-Seoane (2010) conducted N-body simulations to investigate the effects of strong mass segregation (Alexander & Hopman 2009; Keshet et al. 2009) and found that cusps formed in a fraction of a (Maxwellian) relaxation time (Amaro-Seoane & Preto 2011). Gualandris & Merritt (2012) conducted similar computations and found that cores are likely to persist for the dominant stellar popular; intriguingly, cusp formation amongst BHs is quicker, but still takes at least a (Maxwellian) relaxation time. In any case, the time taken to form a cusp depends upon the initial configuration of stars, and so will depend upon the Galaxy's history. The true level of relaxation in the Galactic

[11] Freitag, Amaro-Seoane, & Kalogera (2006) found that using a consistent velocity distribution for the population of stars (from an η-model) instead of relying on the Maxwellian approximation made negligible change to the dynamical friction time-scale. They did not consider a cusp as severe as $p = 0.5$.

centre is uncertain. We cannot add further evidence to settle the matter. For definiteness, we have assumed that a cusp has formed in our calculations.

Despite the long relaxation time-scale, some of the most weakly bound orbits have even longer orbital periods. This only effects orbits with $1 - e < 10^{-3}$. These form a fringe at the edge of region accurately described by the Fokker-Planck cusp solution (Spitzer & Shapiro 1972).

Looking at the relaxation time-scales for individual orbits, we see a consistent picture. Time-scales range by many orders of magnitude. The longest are for the most tightly bound orbits. This reflects that the cusp forms from the outside-in, and that these orbits may not yet be populated, although this will crucially depend upon the initial population of orbits. The shortest time-scales are for the most weakly bound orbits, those with large periapses and eccentricities. The orbital period can be much shorter than these time-scales, again highlighting the fringe where the Fokker-Planck approximation is not appropriate. The variation in the time-scale is likely exaggerated by our neglecting of the spatial variation in the population of stars: tighter bound stars will pass through denser regions, so we may expect their true time-scales to be smaller, while loser bound stars will pass through less dense regions, so we would expect longer time-scales. This is further enhanced by the mass segregation which will increase the average mass of objects further inside the cusp.

When comparing gravitational wave inspiral time-scales and orbital angular momentum time-scales, equality can occur for times far exceeding the Hubble time. This only occurs for lower eccentricities, which are not of interest for bursts, and so this does not concern us for this work. However, it may be interesting to consider the distribution of objects in this region, which is not relaxed but is dominated by gravitational wave inspiral. Since inspiral takes such a huge time to complete, it is possible there is a pocket of objects currently mid-inspiral that reflect the unrelaxed distribution of stars.

APPENDIX B: EVOLUTION OF ORBITAL PARAMETERS FROM GRAVITATIONAL WAVE EMISSION

B1 Bound orbits

For bound orbits it is possible to define a gravitational wave inspiral time from the orbit-averaged change in the orbital parameters. Using the analysis of Peters (1964) for Keplerian binaries, the averaged rates of change of the periapsis and eccentricity are

$$\left\langle \frac{\mathrm{d}r_\mathrm{p}}{\mathrm{d}t} \right\rangle = -\frac{64}{5}\frac{\zeta}{r_\mathrm{p}^3}\frac{(1-e)^{3/2}}{(1+e)^{7/2}}\left(1 - \frac{7}{12}e + \frac{7}{8}e^2 + \frac{47}{192}e^3\right) \tag{B1}$$

$$\left\langle \frac{\mathrm{d}e}{\mathrm{d}t} \right\rangle = -\frac{304}{15}\frac{\zeta}{r_\mathrm{p}^4}\frac{e(1-e)^{3/2}}{(1+e)^{5/2}}\left(1 + \frac{121}{304}e^2\right), \tag{B2}$$

where we have introduced

$$\zeta = \frac{G^3 M_\bullet M (M_\bullet + M)}{c^5}. \tag{B3}$$

For a circular orbit the inspiral time from initial periapsis r_p0 is

$$\tau_\mathrm{c}(r_\mathrm{p0}) = \frac{5}{256}\frac{r_\mathrm{p0}^4}{\zeta}. \tag{B4}$$

For an orbit of finite eccentricity ($0 < e < 1$), we can solve for the periapsis as a function of eccentricity

$$r_\mathrm{p}(e) = \chi(1+e)^{-1}\left(1 + \frac{121}{304}e^2\right)^{870/2299} e^{12/19}, \tag{B5}$$

where χ is a constant fixed by the initial conditions: for an orbit with initial eccentricity e_0

$$\chi = (1+e_0)\left(1 + \frac{121}{304}e_0^2\right)^{-870/2299} e_0^{-12/19} r_\mathrm{p0}. \tag{B6}$$

The inspiral is complete when the eccentricity has decayed to zero. Consequently the inspiral time is (Peters 1964)

$$\tau_\mathrm{insp}(r_\mathrm{p0}, e_0) = \int_0^{e_0} \frac{15}{304}\frac{\chi^4}{\zeta}\frac{e^{29/19}}{(1-e^2)^{3/2}}\left(1 + \frac{121}{304}e^2\right)^{1181/2299} \mathrm{d}e. \tag{B7}$$

This is best evaluated numerically, but it may be written in closed form as

$$\tau_\mathrm{insp}(r_\mathrm{p0}, e_0) = \tau_\mathrm{c}(r_\mathrm{p0})(1+e_0)^4\left(1 + \frac{121}{304}e_0^2\right)^{-3480/2299} F_1\left(\frac{24}{19}; \frac{3}{2}, -\frac{1181}{2299}; \frac{43}{19}; e_0^2, -\frac{121}{304}e_0^2\right), \tag{B8}$$

using the Appell hypergeometric function of the first kind $F_1(\alpha; \beta, \beta'; \gamma; x, y)$ (Olver et al. 2010, 16.15.1).[12]

[12] For small eccentricities $\tau(r_\mathrm{p0}, e_0) \simeq \tau_\mathrm{c}(r_\mathrm{p0})[1 + 4e_0 + (273/43)e_0^2 + \mathcal{O}(e_0^3)]$.

B2 Unbound orbits

Unbound orbits only pass through periapsis once. We therefore expect that their evolution through the loss of energy and angular momentum carried away by gravitational waves to be small. Following the approach of Turner (1977) we can calculate the change in the eccentricity and periapse of an unbound Keplerian binary. The change in fractional eccentricity over an orbit, approximating the orbital parameters remain constant throughout, is

$$\frac{\Delta e}{e} = -\frac{608}{15}\Sigma\left[\frac{1}{(1+e)^{5/2}}\left(1+\frac{121}{304}e^2\right)\cos^{-1}\left(-\frac{1}{e}\right)+\frac{(e-1)^{1/2}}{e^2(1+e)^2}\left(\frac{67}{456}+\frac{1069}{912}e^2+\frac{3}{38}e^4\right)\right], \tag{B9}$$

introducing dimensionless parameter

$$\Sigma = \frac{G^{5/2}M_\bullet M(M_\bullet+M)}{c^5 r_{\rm p}^{5/2}}. \tag{B10}$$

Similarly, the fractional change in periapsis is

$$\frac{\Delta r_{\rm p}}{r_{\rm p}} = -\frac{128}{5}\Sigma\left[\frac{1}{(1+e)^{7/2}}\left(1-\frac{7}{12}e+\frac{7}{8}e^2+\frac{47}{192}e^3\right)\cos^{-1}\left(-\frac{1}{e}\right)-\frac{(e-1)^{1/2}}{e(1+e)^3}\left(\frac{67}{288}-\frac{13}{8}e+\frac{133}{576}e^2-\frac{1}{4}e^3-\frac{1}{8}e^4\right)\right]. \tag{B11}$$

Both of these changes obtain their greatest magnitudes for large eccentricities, then

$$\frac{\Delta e}{e} \simeq \frac{\Delta r_{\rm p}}{r_{\rm p}} \simeq -\frac{16}{5}\Sigma e^{1/2}. \tag{B12}$$

For extreme mass-ratio binaries, as is the case here, the mass-ratio is a small quantity

$$\eta = \frac{M}{M_\bullet} \ll 1. \tag{B13}$$

The smallest possible periapsis is of order of the Schwarzschild radius of the MBH, such that

$$r_{\rm p} = \alpha\frac{GM_\bullet}{c^2}; \quad \alpha > 1. \tag{B14}$$

These give

$$\Sigma = \frac{\eta}{\alpha^{5/2}} < \eta \ll 1. \tag{B15}$$

Hence the changes in orbital parameters will be significant for

$$e \sim \frac{25}{256}\frac{\alpha^5}{\eta^2} > \frac{25}{256}\frac{1}{\eta^2}. \tag{B16}$$

Such orbits should be exceedingly rare, and so it is safe to neglect inspiral for unbound orbits.

This paper has been typeset from a TEX/ LATEX file prepared by the author.